AFRL-VS-TR-2003-1594

VALIDATION OF IONOSPHERIC MODELS

Patricia Doherty

Boston College
Institute for Scientific Research
140 Commonwealth Avenue
Chestnut Hill, MA 02467-3862

31 March 2003

Scientific Report No. 7

20040204 172

AIR FORCE RESEARCH LABORATORY
Space Vehicles Directorate
29 Randolph Rd
AIR FORCE MATERIEL COMMAND
Hanscom AFB, MA 01731-3010

"This technical report has been reviewed and is approved for publication"

/signed/   /signed/

_____   _____
JOHN RETTERER   ROBERT MORRIS
Contract Manager   Branch Chief

REPORT DOCUMENTATION PAGE

The public reporting burden for this collection of information is estimated to average 1 hour per response, including the time for reviewing instructions, searching existing data sources, gathering and maintaining the data needed, and completing and reviewing the collection of information. Send comments regarding this burden estimate or any other aspect of this collection of information, including suggestions for reducing the burden, to Department of Defense, Washington Headquarters Services, Directorate for Information Operations and Reports (0704-0188), 1215 Jefferson Davis Highway, Suite 1204, Arlington, VA 22202-4302. Respondents should be aware that notwithstanding any other provision of law, no person shall be subject to any penalty for failing to comply with a collection of information if it does not display a currently valid OMB control number.
PLEASE DO NOT RETURN YOUR FORM TO THE ABOVE ADDRESS.

1. REPORT DATE (DD-MM-YYYY)	2. REPORT TYPE	3. DATES COVERED (From - To)
31-03-2003	Scientific Report No. 7	April 2002 - March 2003

4. TITLE AND SUBTITLE	5a. CONTRACT NUMBER
VALIDATION OF IONOSPHERIC MODELS	F19628-96-C-0039
	5b. GRANT NUMBER
	5c. PROGRAM ELEMENT NUMBER 61102F

6. AUTHOR(S)	5d. PROJECT NUMBER 1010
Patricia H. Doherty	5e. TASK NUMBER IM
	5f. WORK UNIT NUMBER AC

7. PERFORMING ORGANIZATION NAME(S) AND ADDRESS(ES)	8. PERFORMING ORGANIZATION REPORT NUMBER
Boston College / Institute for Scientific Research 140 Commonwealth Avenue Chestnut Hill, MA 02467-3862	

9. SPONSORING/MONITORING AGENCY NAME(S) AND ADDRESS(ES)	10. SPONSOR/MONITOR'S ACRONYM(S)
Air Force Research Laboratory/VSBXP 29 Randolph Road Hanscom AFB, MA 01731-3010	
	11. SPONSOR/MONITOR'S REPORT NUMBER(S) AFRL-VS-TR-2003-1594

12. DISTRIBUTION/AVAILABILITY STATEMENT

Approved for public release; distribution unlimited.

13. SUPPLEMENTARY NOTES

14. ABSTRACT

During the period of April 2002 through March 2003, we have continued to pursue the validation of ionospheric models. This work included significant efforts to access, process and analyze Total Electron Content (TEC) data from a variety of sources. These databases were useful in a series of validation studies that focused on PRISM's ability to predict the sub-peak ionospheric profile and geomagnetic storm effects. They were also useful in determining the overall quality of data from several sources. In this year, we also finalized two major projects. These projects included the validation of the GPS Single-Frequency Position Maps and the development of a pre-processor for PRISM that will enable the assimilation of a new source of ionospheric data from the UltraViolet (UV) imagers of the impending DMSP Block 5D-3 satellites. The work summarized above resulted in four presentations at various ionospheric conferences, three papers published in meeting proceedings and two AFRL Technical Reports.

15. SUBJECT TERMS

Parameterized Real-Time Ionospheric Specification Model (PRISM), Total Electron Content (TEC), Wide Area Augmentation System (WAAS), OPerational Space Environment Network Display (OP-SEND), foF2 (peak F2 region operating frequency), hmF2 (peak height of the F2 region), ymF2 (half-thickness of the F2 region)

16. SECURITY CLASSIFICATION OF:			17. LIMITATION OF ABSTRACT	18. NUMBER OF PAGES	19a. NAME OF RESPONSIBLE PERSON
a. REPORT	b. ABSTRACT	c. THIS PAGE			John Retterer
U	U	U	SAR		19b. TELEPHONE NUMBER (Include area code) 781-377-3891

TABLE OF CONTENTS

LIST OF FIGURES

1. GOALS

The objective of this contract is to obtain ionospheric measurements from a wide range of geographic locations and to utilize the resulting databases to validate the theoretical ionospheric models that are the basis of the Parameterized Ionospheric Specification Model (PRISM) and the Ionospheric Forecast Model (IFM).

In this past year, we have supported these goals with the following activities:

- Obtained and analyzed TEC measurements from a variety of sources for use in PRISM.
- Finalized Validations of the GPS Single Frequency Position Error Maps.
- Performed TEC studies designed to test quality of data effects in PRISM.
- Performed validations of PRISM sub-peak profiles.
- Tested the PRISM validation tool.
- Tested PRISM's ability to reproduce geomagnetic storm effects.
- Finalized the development of software to merge real-time ionospheric UV measurements for use in the PRISM model.

2. PROGRESS

2.1 Data Acquisition and Analysis

Significant data processing and analysis was performed in the current year. The data sets include Total Electron Content (TEC) data from a variety of sources including the following:

- International GPS Geodetic System Network (IGS)
- Jet Propulsion Laboratory (JPL)
- TOPEX/POSEIDON mission satellite
- Wide Area Augmentation System (WAAS).

The WAAS data is a new source of highly accurate TEC available for modeling studies at AFRL. WAAS is a GPS satellite-based navigation system maintained by the Federal Aviation Administration. The system provides optimized ionospheric corrections for single-frequency GPS users over the CONtiguous U.S. (CONUS). The corrections are based on a network of GPS receivers placed at 24 reference stations over the CONUS. A master station utilizes the receiver data from all the reference sites to provide a grid of ionosphere corrections at 5° increments over the CONUS region. Single-frequency aircraft users obtain the grid of corrections from a geostationary satellite message and interpolate a local ionospheric correction from the nearest available grid points. The interpolation is weighted by the estimated grid point errors, also provided by the WAAS system. For each of the 24 measurement stations of WAAS, there are three identical receivers. In the WAAS process, the data from all three receivers are compared for

receiver bias estimation and data quality control. This redundancy in processing results is a highly accurate near real-time ionospheric estimation in the CONUS.

The use of WAAS TEC together with the other TEC sources listed above required the development of a variety of processing algorithms and graphics development. These data analysis efforts allowed us to utilize high quality data in a series of studies that are described in this report.

2.2 Validations of the GPS Single-Frequency Error Maps

In the current year, we have finalized validation of the OpSEND Estimated Single-Frequency Position Error Maps that are produced operationally for the Air Force 55th Space Weather Squadron. These maps estimate the position errors that result from inaccurate ionospheric corrections for the GPS single-frequency user. The original software that produces these maps of position errors was developed in an earlier period of this contract. It determines the errors by using the slant TEC from the PRISM model. The utility of these maps is highly dependent on the accuracy of PRISM and the fact that the error budget for single-frequency determined positions is dominated by the range delay caused by the ionosphere.

This year we completed validation for the maps at a mid- and high-latitude location and provided documentation that is included in an AFRL technical report (Decker, D.T., Doherty, P.H., Bishop, G.B, Holland, E., Andreason, A.K., Andreason, C.C., Xu, T., and Scro, K.D., "Validation of OpSEND – Estimated GPS Single Frequency Error Maps," AFRL Technical Report, February 2003).

The mid-latitude location was the Hanscom AFB site. Single frequency GPS measurements at the Hanscom AFB site were initiated on 3 January 2001 and continued through the end of July 2001 (excluding late March to 19 April). This site was selected to represent mid-latitude performance for the GPS Error Map product. Approximately three weeks of data recorded within the measurement period were selected for processing. These days were selected to represent single frequency measurement in 2001 and model performance for three different seasons. The selected days include: 21-28 January, 11-12 February (10 days of Winter), 22-28 April (7 days of Equinox), 22-25 June, 28 June, 11 July, 21 July (7 days of Summer). Geomagnetic activity levels during the validation periods were quiet to moderate.

The single frequency measurements at Hanscom were recorded at 5Hz from the roof of one of the buildings at AFRL. This site is located at 42.45404° North, 71.27274° West and 56.787 meters above sea level. These measurements were recorded at a 5Hz rate with a Trimble Pathfinder single frequency GPS receiver. This receiver is a civil receiver with Standard Positioning System performance accuracy. The output from the receiver includes the universal time, the position solution (latitude, longitude and altitude), Position Dilution of Precision (PDOP) and the Pseudo Random Noise numbers (PRN) of the satellites used in the calculations.

A sample of the single frequency measurements recorded at Hanscom during the winter season (21 January) is illustrated in Figures 1 and 2. In the top panel of Figure 1, we show the PRN's used to calculate position. Lower panels include the PDOP, Latitude Error (m), Longitude Error (m) and Height Error (m). Figure 2 displays the resultant 2D (latitude and longitude) and 3D (latitude, longitude and altitude) position errors. Note that the data displays frequent gaps in coverage together with higher than expected PDOP values. This behavior was illustrated in all of the winter measurements. Samples of the data recorded in the equinox and summer seasons are shown in Figures 3 through 6, with Figures 3 and 4 representing the equinox measurements and Figures 5 and 6 displaying results for the summer season. A comparison of the sample data from the three seasons illustrates that the anomalous behavior of the January data do not occur in either of the other two seasons. We currently believe that the behavior in January was related to antenna problems because after the antenna configurations were modified in late March and early April the anomalous behavior no longer appeared.

Examination of the Hanscom data shows many of the same features as were seen at Ascension Island. Ascension Island results were presented in last year's annual report. The magnitude of the Hanscom errors are generally smaller than what was seen at Ascension Island. For example, in Figure 4 we see that the maximum 2D error was around 9 meters with most of the error falling easily below 6 meters. The 3D error peaks around 13 meters and mostly falls below 10 meters. The daily mean of the 2 and 3D errors shown in Figure 4 are 2.3 and 4.74 respectively. These values are in contrast to Ascension Island where the sample equinox day exhibited errors that peaked at approximately 30 and 60 meters for the 2D and 3D errors and 2D daily means of 7.56m and 3D daily means of 16.9m and errors peaked at around 30 and 60 meters.

Single frequency GPS measurements at the high-latitude site at HAARP in Alaska were initiated on 19 April 2001 and continued to early October 2001. This site was selected to represent high-latitude performance for the GPS Error Map product. Two weeks of data recorded within the measurement period were selected for processing. These days were selected to represent single-frequency measurement and model performance for two different seasons in 2001. The selected days include: 21 April , 24-26 April, 2,4 and 8 May (7 days during Equinox), 13-16 June, 23-25 June (7 days in Summer). Geomagnetic activity levels during the validation periods were quiet to moderate.

The single frequency measurements at the HAARP site were recorded at 5Hz from 62.39911° North, 145.15757° West and 599.461 meters above sea level. These measurements were made with a Trimble Pathfinder single frequency receiver with Standard Positioning System performance accuracy. The output from the receiver includes the universal time, the position solution (latitude, longitude and altitude), PDOP and the PRN's of the satellites used in the calculations.

A sample of the single frequency measurements recorded at HAARP during the equinox season is illustrated in Figures 7 and 8. In the top panel of Figure 7, we show the PRNs of the satellites used to calculate the position. Similar to the Hanscom receiver, more than 4 satellites appear to be used for position determination. Lower panels include the

3

PDOP, Latitude Error (m), Longitude Error (m) and Height Error (m). Figure 8 displays the resultant 2D (latitude and longitude) and 3D (latitude, longitude and height) position errors. These figures illustrate 2D errors in the range of .2-10 meters, with a mean of 1.98 meters. The 3D errors range between .5 and 16 meters, with an overall mean of 4.07 meters. Figures 9 and 10 include sample measurements for the summer season, where 2D errors range between .1 and 8 meters, with a mean of 1.44 meters. 3D errors range between 1 and 12 meters, with a mean of 3.77 meters. These are essentially similar size errors to those being seen at Hanscom.

We found that the measurements recorded on June 25th showed some poor data quality between 2 and 8UT. Since we cannot account for the source of this anomalous behavior, we have eliminated the data from this period in our analysis. Other than this anomalous period, Figures 7 through 10 represent the overall behavior of the measurements at this high latitude location.
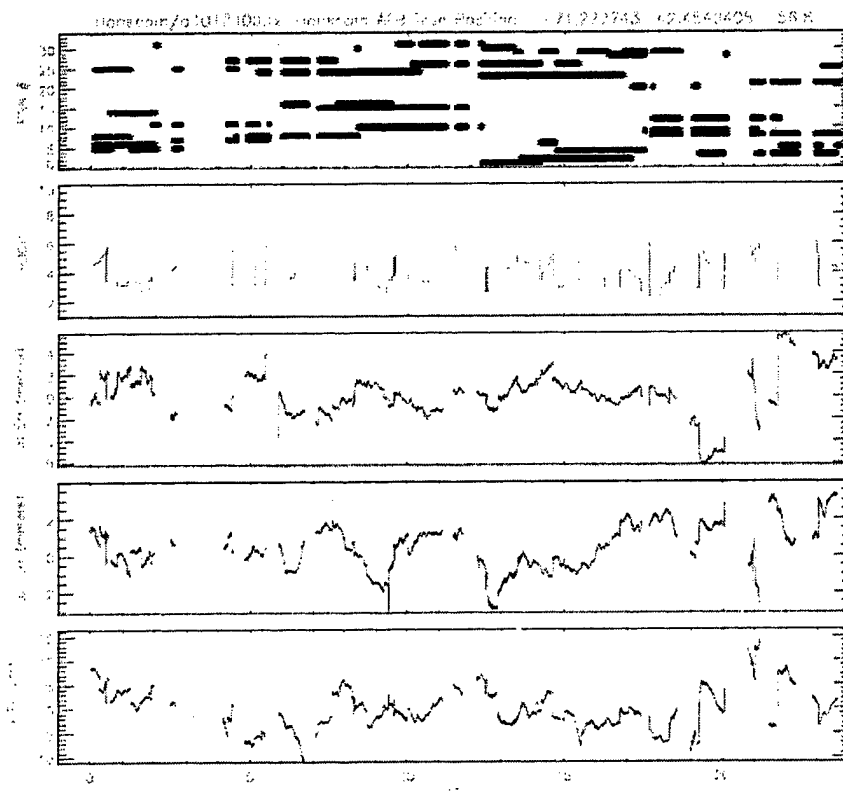
Figure 1. Single-frequency Measurements and 1D Errors Recorded at Hanscom 1/21/01.
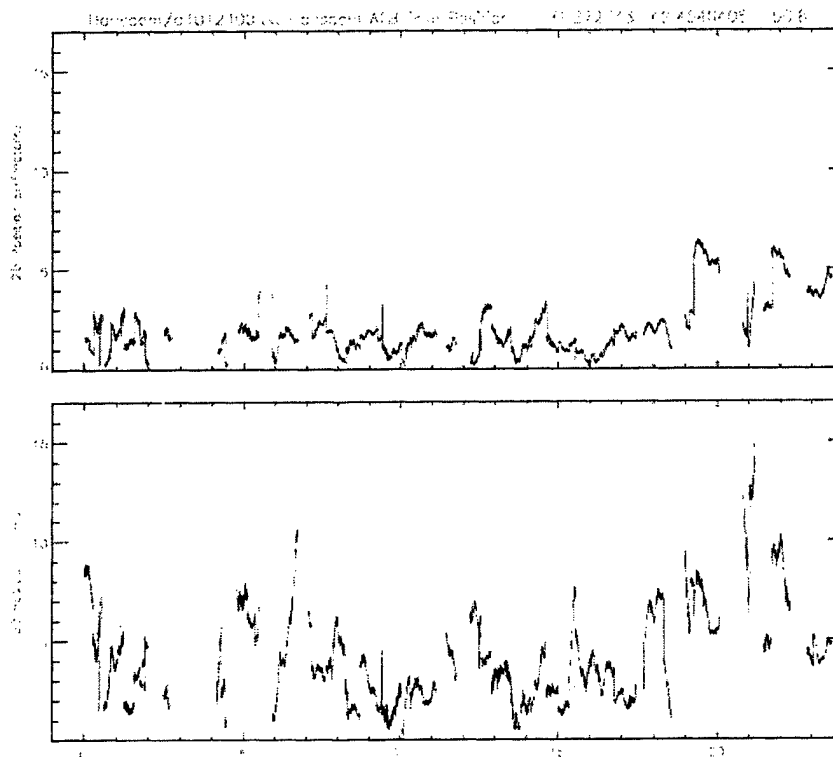

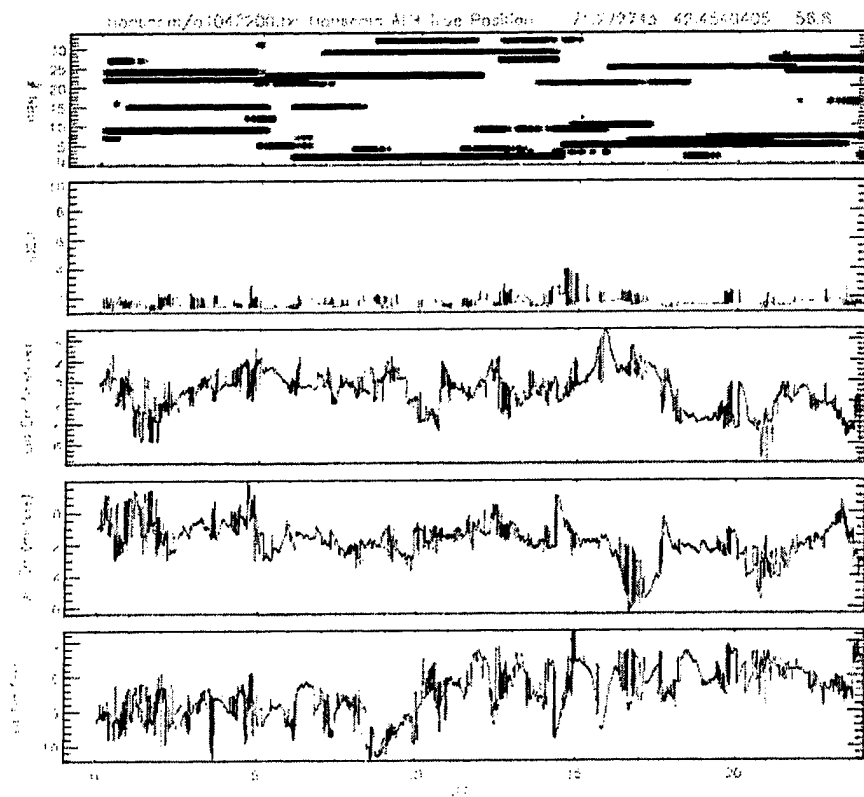Figure 2. 2D and 3D Position Errors Recorded at Hanscom 1/21/01.

Figure 3. Single-frequency Measurements and 1D Errors Recorded at Hanscom 4/22/01.

Figure 4. 2D and 3D Position Errors Recorded at Hanscom 4/22/01.

Figure 5. Single Frequency Measurements and 1D Errors Recorded at HAFB, 6/22/01.
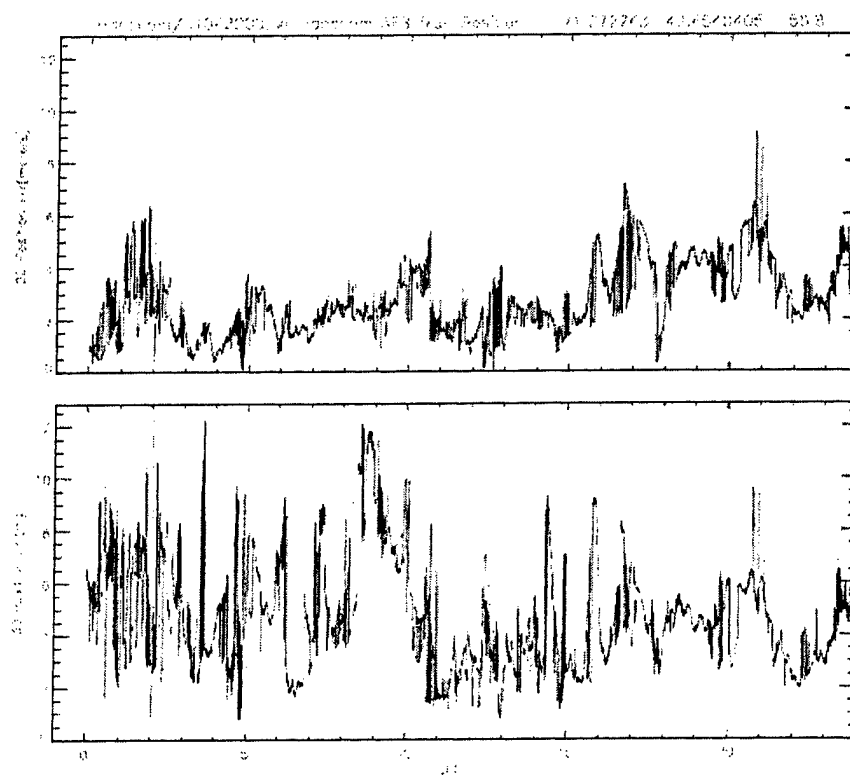
Figure 6. 2D and 3D Position Errors Recorded at HAFB, 6/22/01.

Figure 7. Single Frequency Measurements and 1D Errors Recorded at HAARP 4/26/01.

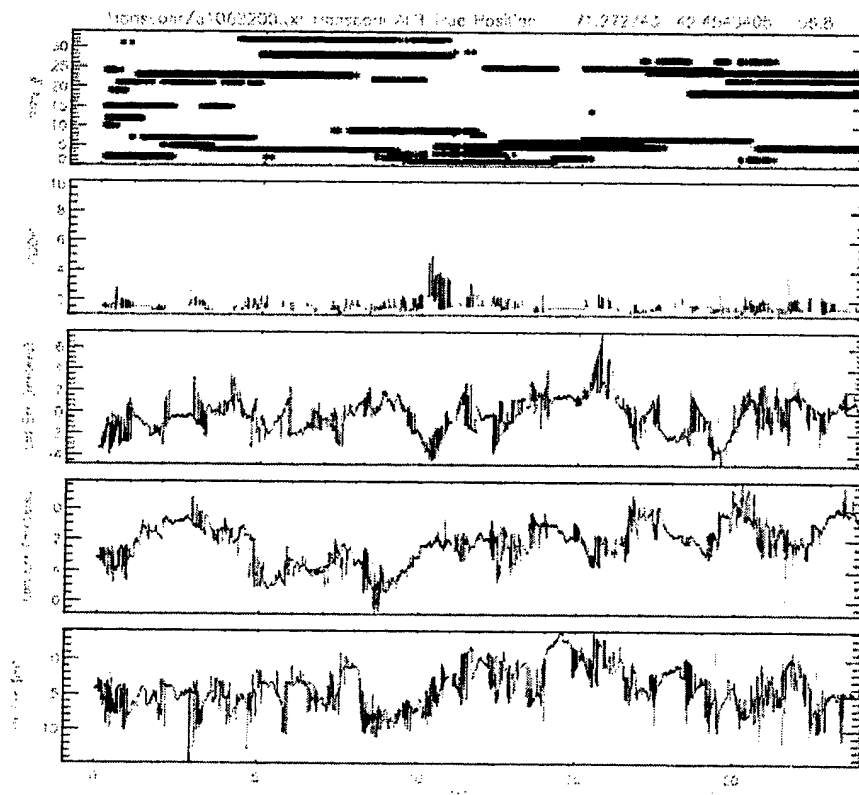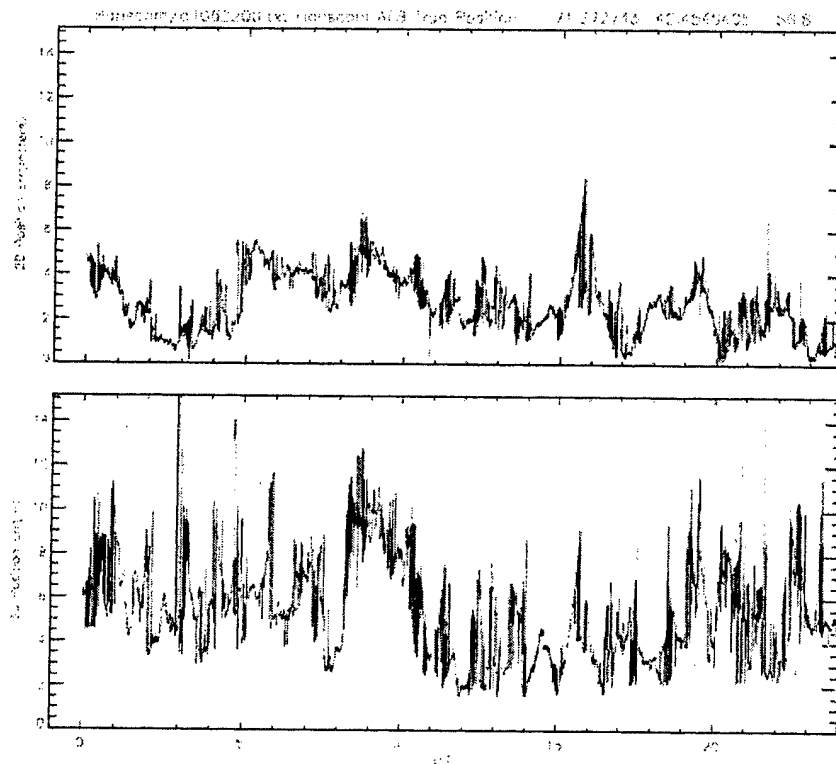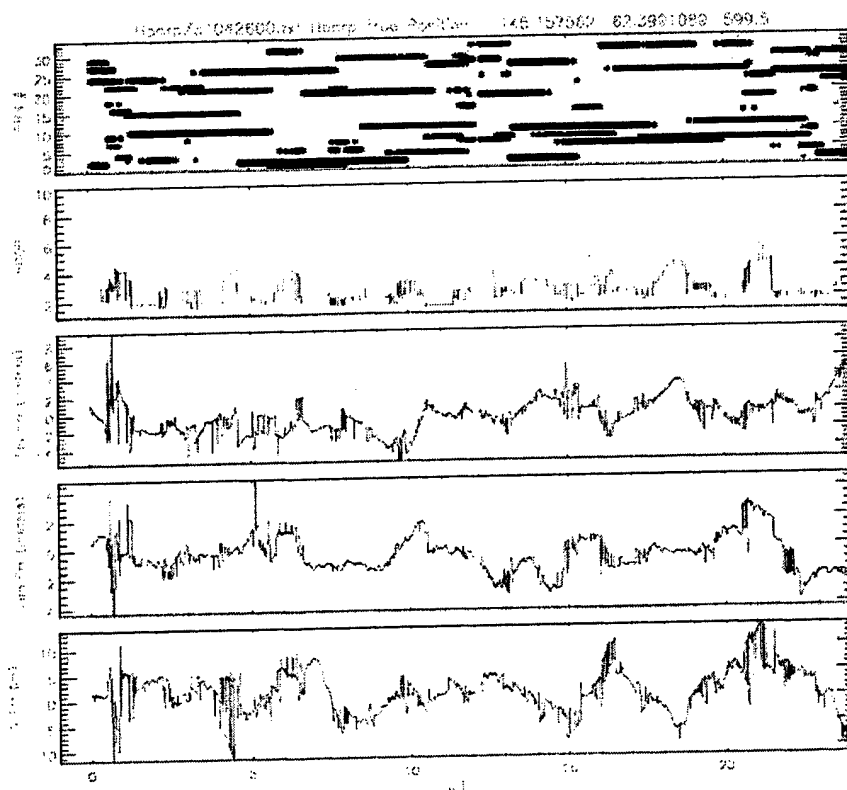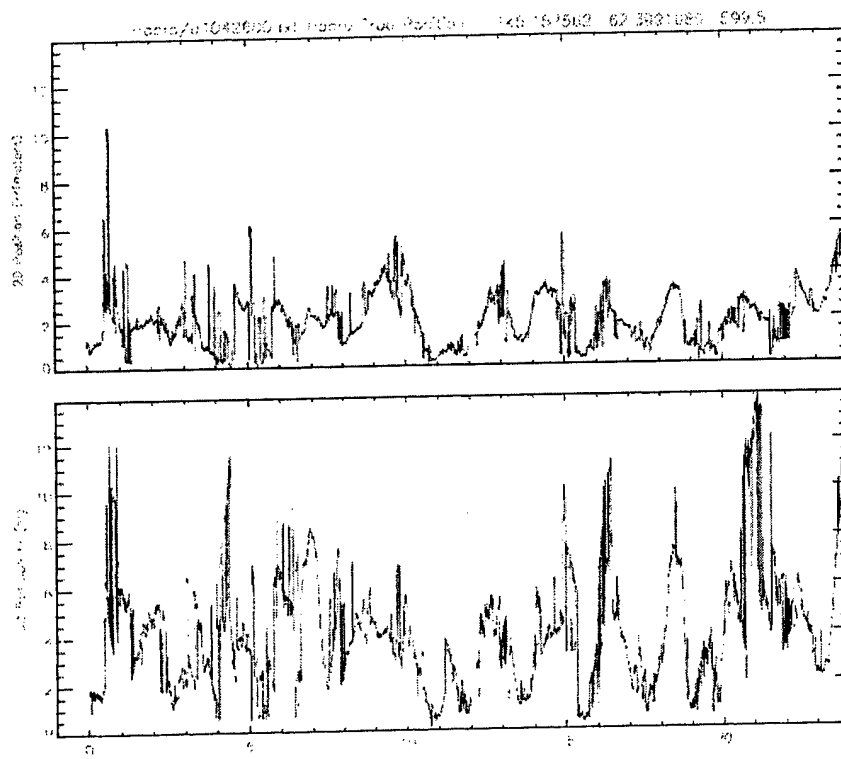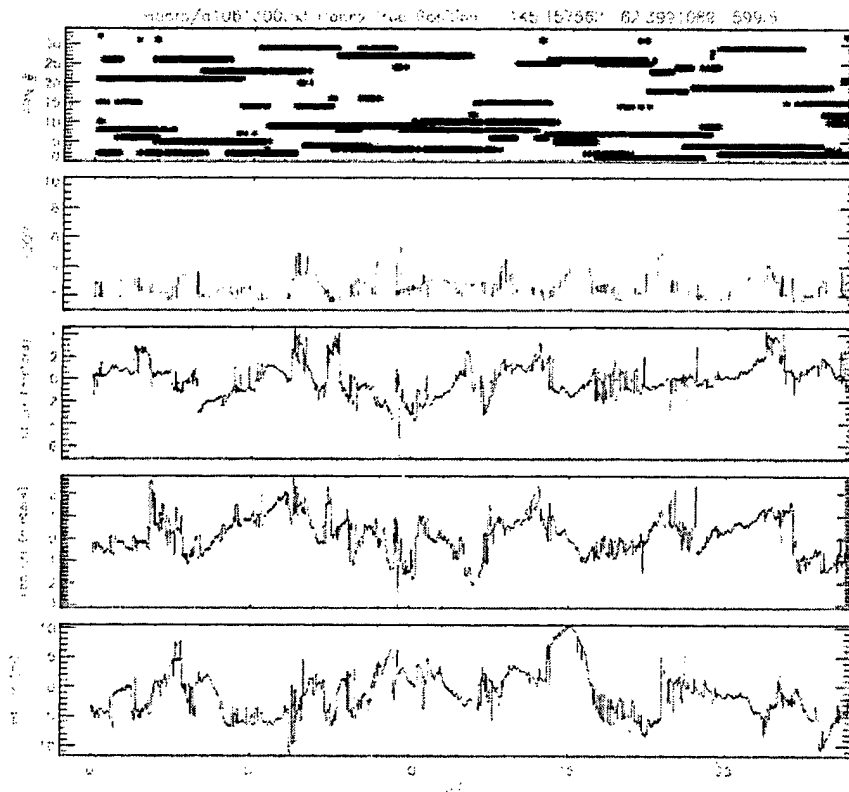Figure 8. 2D and 3D Position Errors Recorded at HAARP 4/26/01.

8

Figure 9. Single-frequency Measurements and 1D Errors Recorded at HAARP 6/13/01.
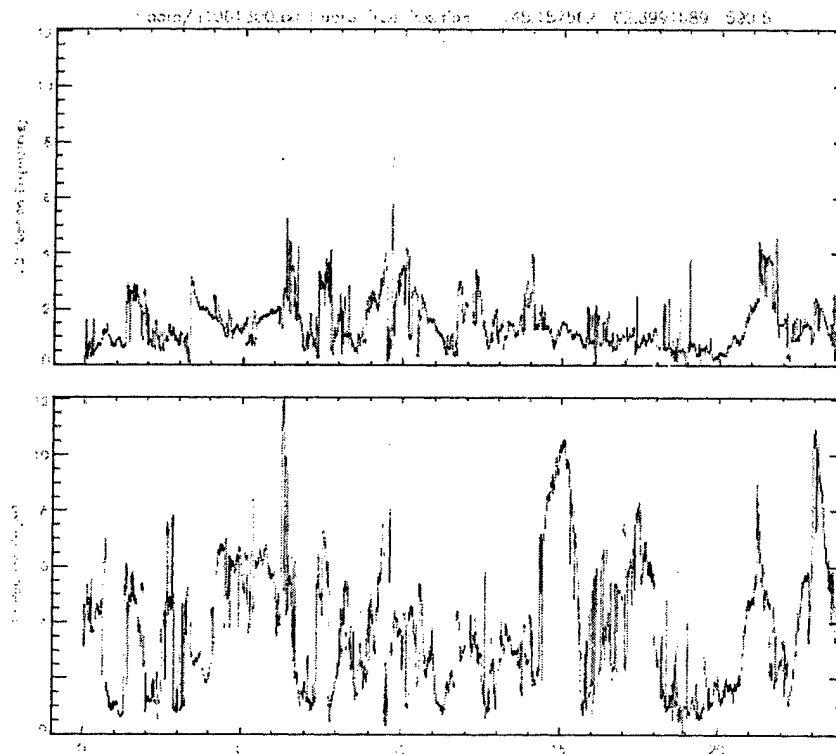
Figure 10. 2D and 3D Position Errors Recorded at HAARP 6/13/01.

2.3 Comparisons of TEC Observations from Collocated Systems

Using the near real-time TEC data from JPL, we compared simultaneous observations of slant TEC from collocated systems. The report is appended to this document (McNamara, L.F., "Comparisons of TEC Observations from Collocated Systems", March 2003) (see Appendix A).

2.4 Validating the PRISM Profile

Efforts were made to validate the sub-peak or bottomside density profiles generated by PRISM in its real-time adjustment mode. The input used in these validations were observations of foF2 (peak F2 layer frequency) and hmF2 (peak height of the F2 layer). PRISM results were compared with the profile processed by the ARTIST program. The comparisons were made for one low-latitude station and one mid-latitude location for the first half of 2002. The results show that the PRISM half-thickness (ymF2) tracks that of the ARTIST values fairly well. A full description of this study is included in a report appended to this document (McNamara, L.F., "Validating the PRISM Profile," April 2002) (see Appendix B).

2.5 Testing the GPS Error Maps and the PRISM Validation Tools

In the current year, we spent time testing the validation tools that were designed by AFRL and RADEX. These tools were developed to enable automated validations of models by Air Force personnel at the 55th Space Weather Squadron. The GPS Error Map tool tests required the development of scripts and graphics techniques to run and display the results. The PRISM tool tests required similar efforts. Case studies were run and provided to AFRL for further testing and analysis.

2.6 Geomagnetic Storm Characterization with PRISM

Different TEC data sets were used with F-region maximum density and height as input to PRISM during a period of severe geomagnetic storm activity. The data processed and prepared for this work included TEC from the near real-time hourly TEC from JPL, the IGS system and WAAS. It also included F-region maximum densities and height together with DMSP high-latitude particles and auroral boundaries. The results showed that the model accuracy in regions where there is no input data is significantly improved as compared to climatology, thus providing confidence in the global model output.

2.7 Ultra-Violet (UV) PRISM Pre-Processor

A product was developed to merge real-time ionospheric observations from different instruments for use in the PRISM model. In last year's annual report, we described the development of this product. In the current year, we performed a series of studies that determined the optimum way to merge the data with other measurements for maximum benefit to PRISM ionospheric specification.

10

The data set that we are attempting to merge with other real-time measurements for PRISM comes from two Ultra-Violet (UV) sensors under development for the DMSP Block 5D-3 satellites. These sensors are named the Special Sensor Ultraviolet Limb Imager (SSULI) and the Special Sensor Ultraviolet Spectrographic Imager (SSUSI). Both are remote-sensing instruments that measure UV emissions emitted by the Earth's upper atmosphere. The studies performed in the current year used the same simulated data described in last year's annual report, but introduced random and systematic errors into the data, and allows for multiple options and scenarios.

A major contribution this year was the development of techniques to decimate the UV data before it is passed to PRISM. Decimating the data permits a study of how data from different sensors should be integrated. PRISM treats all data as equally valid, which means that large sets of satellite data would completely swamp the more limited ground-based DISS data, for example, which is generally more reliable than the indirect satellite observations. Even the UV data raises this issue, since the UV data will be more voluminous from the SSUSI data than the SSULI data, and would therefore swamp the SSULI data if all observations were simply passed together to PRISM.

Other efforts supporting the UV Prism Pre-Processor development were an investigation of how to combine the satellite and ground-based ionospheric observations. Techniques were tested that increased the weight of a particular ground-based observation, to see if this is a good procedure for applying relative weights to different ground locations.

In the current year, we finalized our efforts in this project and documented the software, testing and results. That documentation will be included in an AFRL Technical Report (Decker, D.T, McNamara, L.F., and Doherty, P.H., "UV-driven PRISM," AFRL Technical Report, in progress).

3. PRESENTATIONS and PUBLICATIONS

Bishop, G., Bullett, T., Groves, K., Quigley, S., **Doherty**, P., Sexton, E. Scro, Wilkes, R. and Citrone, P., "Operational Space Environment Network Display (OpSEND)," presented to the Ionospheric Effects Symposium 2002, Alexandria, VA, May 2002. This paper was also published in the Proceedings of IES 2002, September 2002.

Bishop, G., Decker, D., Sexton, E., **Doherty**, P., de la Braujardiere, O., Bullett, T., Quigley, S. and Groves, K., "Space Weather Model and Product Validation," presented to the Ionospheric Effects Symposium 2002, Alexandria, VA, May 2002. This paper was also published in the Proceedings of IES 2002, September 2002.

McNamara, L.F., VHF Transequatorial Propagation and Equatorial Bubbles," presented to the Ionospheric Effects Symposium 2002, Alexandria, VA, May 2002. This paper was also published in the Proceedings of IES 2002, September 2002.

O. de la Beaujardiere, D.Decker, F. Rich, J. Retterer, W. Burke, B. Basu, T. Bullett, G. Crowley, M. Kelley, J. Makela, **L. McNamara**, C.Huang and **P. Doherty**, "The global ionosphere during the April 17 to 20, 2002 Magnetic Storm", presented as an invited talk to Fall AGU, San Francisco, CA, December 2002.

4. TECHNICAL REPORTS

Decker, D.T., Doherty, P.H., Bishop, G.B, Holland, E., Andreason, A.K., Andreason, C.C., Xu, T., and Scro, K.D., "Validation of OpSEND – Estimated GPS Single Frequency Error Maps," AFRL Technical Report, February 2003.

Decker, D.T, McNamara, L.F., and Doherty, P.H., "UV-driven PRISM," AFRL Technical Report, in progress.

APPENDIX A

Comparisons of TEC Observations from Collocated JPL Systems

March 2003

Summary

There are three stations for which JPL runs two parallel systems, Goldstone, California, Tidbinbilla, S.E. Australia, and Madrid, Spain. Simultaneous observations of slant TEC by the two systems have been compared in detail, in order to provide representative error bars for these as well as other observations.

As with any observations, the observed values must be accompanied by an estimate of the uncertainty in the measurement process. JPL provides estimates of these errors, which are usually less than ~1 TECU, for both vertical and oblique values of TEC.

Since the accuracy of the GPS navigation depends on the differences between pairs of slant TEC measurements, the estimated errors in each observation (in TECU) must be added to provide the error estimate for the values of ΔTEC. Taking the JPL error estimate of 1 TECU gives an uncertainty of 2 TECU in values of ΔTEC.

The differences between simultaneous observations of TEC for each station pair have been analyzed in some detail. The results can be summarized in terms of the weighted diurnal average of the average and RMS discrepancies between corresponding observations at each local time. The results for September 2002 are given in *Table A-1*.

Table A-1: Diurnal Averages of the Average and RMS Discrepancies at each LT Hour.

Station	Average	RMS
Goldstone	-1.63	2.66
Madrid	-0.70	1.92
Tidbinbilla	-0.03	3.80

In the interests of providing a single representative value for the error, we can assume that these (September 2002) results are representative of the three stations, and set the average RMS error to the highest value, ~4 TECU. This corresponds to an RMS error of ~2 TECU in the values of slant TEC. Note that nothing can be said about any systematic errors at a given station.

The RMS uncertainties at other JPL sites can be expected to be higher than 2 TECU, since this is the value for an ideal situation in which significant differences between simultaneous observations will highlight problems with at least one of the two systems, and lead to their being fixed.

Higher uncertainties must be attributed to isolated stations, since it is much harder to ensure that the absolute values of TEC are correct, as exemplified by the very large systematic errors found by AFRL in the PIMO (Philippines), ZWEN (Russia) and PERT (Australia) observations.

Introduction

Simultaneous observations of slant TEC by two collocated systems operated by JPL have been compared in detail, in order to provide representative error bars for the observations. JPL provides error bars in the data that it sends to AFRL in near real-time, but these seem to be more theoretical than practical.

The need to specify the uncertainties in TEC observations is particularly acute for applications that involve the differences between the values of TEC obtained from multiple satellites. In fact, it has been shown by Greenspan et al[1] (1991) in a linearized solution to the navigation equations that the accuracy of the navigation solution depends on the differences between the ionospheric time delays to a receiver from different GPS satellites, rather than on the absolute values of those delays.

When ΔTEC values are determined, the individual absolute errors must be added to get the error in the difference. This means, for example, that a 2 TECU uncertainty in the observations leads to a 4 TECU discrepancy in the difference between two values.

The agreement or otherwise between TEC observations from different networks such as JPL, WAAS, TOPEX and CORS, is not addressed here. The interest here is how well the slant TECs observed by two collocated systems of the same network agree when they are made simultaneously. This is close to the ideal situation, for which the discrepancies between two systems should essentially be zero. If they are not, the discrepancies will provide the minimum possible errors in the TEC observations.

A similar, but less detailed, analysis of collocated JPL observations has been reported earlier, in the report *Procedures for Quality Control of TEC Observations*. Because of the way in which the quality control procedures evolved, the comparison was between individual values of the TEC relative to an approximate monthly median. RMS errors of 2 to 3 TECU were illustrated in that report.

For the results presented here, the simultaneous observations using two systems have been compared record by record. Three JPL sites lend themselves to this type of analysis

1.   Goldstone, California (GOL2, GOLD)

2.   Madrid, Spain (MAD2, MADR)

3.   Tidbinbilla, S.E. Australia (TID2, TIDB)

The procedures established have been described in a separate report (*Detailed Comparisons of JPL Values of TEC from Collocated Sites - Method*), so only the results are presented here. The procedures can in principle be run for any month for which AFRL has TEC data from JPL, but only a single month is considered here. More

---

[1] Greenspan, R.L., A.K.Tetwsky, J.I.Donna, and J.A.Klobuchar (1991): *The effects of ionosperic errors on single-frequency GPS users.* ION GPS-91 Proceedings.

extensive statistics could be derived by running the Fortran program
compare_colocated_slantTECs.for under the control of a Unix script.

The results for Tidbinbilla are presented first because they have the largest level of inconsistency.

Note: Detailed explanations of the cause of the discrepancies are not offered here, since the causes probably lie in the engineering details of the GPS receivers.

Tidbinbilla

The results of the comparisons are presented in terms of the LSF straight line relating the corresponding values of TEC, and as six plots that illustrate the differences in various ways. *Table A-2* shows the statistical results for Tidbinbilla, September 2002. (The number of significant figures is too high in this table, but the correlation coefficients need to have three figures.)

Table A-2: Statistics of LSF Straight Line, Tidbinbilla, September 2002

Parameter	Value
Sample size (month)	3561
Slope of LSF line	0.95
Intercept of LSF line	2.06
Average TEC1 (TID2)	38.84
Average TEC2 (TIDB)	38.81
Correlation coefficient	0.98
Weighted diurnal average	-0.03
Weighted RMS discrepancy	3.80

The LSF line relating the two TECs is

$$TIDB = 0.946 \ TID2 + 2.062,$$

with a sample size of 3561 and a correlation coefficient of 0.984. Ideally, the slope would be one, and the intercept zero.

The weighted diurnal average of -0.03 is consistent with the difference between the average values, 38.843 and 38.809. The TIDB results (TEC2) are 0.03TECU lower than the TID2 (TEC1, the reference) values. It is hard to imagine a smaller net observational error.

The weighted diurnal RMS error of 3.80 TECU is more representative of the discrepancies, since the average is "over-sold" by the cancellation of positive and negative discrepancies.

Figure A-1 show the diurnal variation of the TID2 values of TEC (on the left), and the TIDB value of TEC versus the TID2 value (on the right).
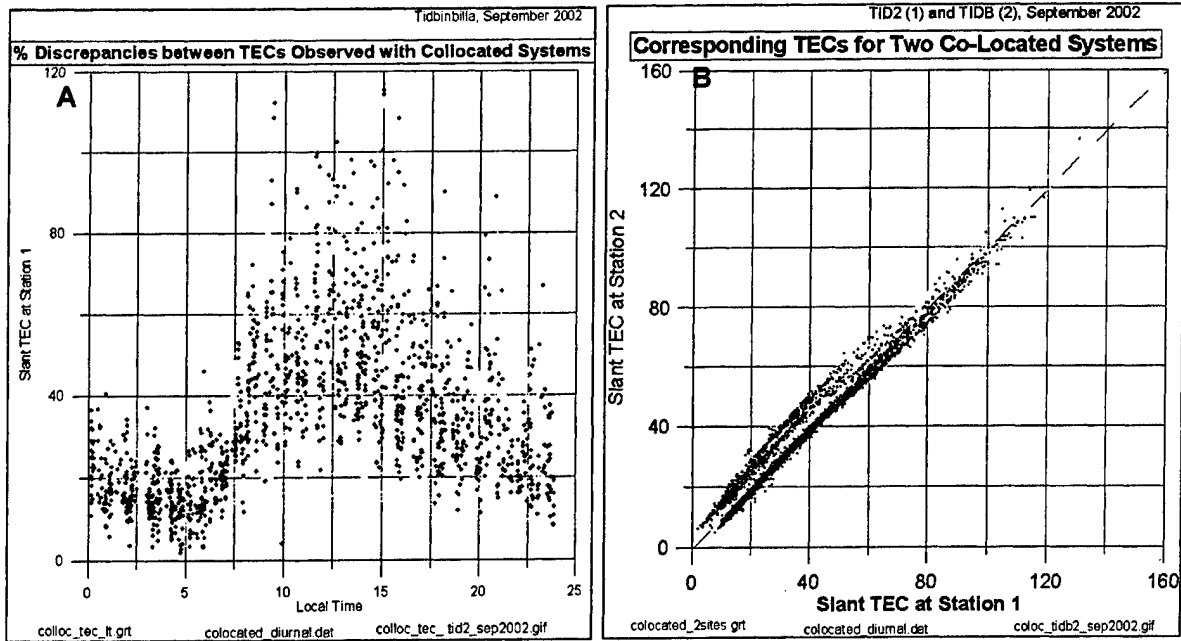
Figure A-1: Diurnal Averages of the Average and RMS Discrepancies at each LT Hour.

The left-hand panel sets the scene, in that it shows both the diurnal variation of the slant TEC observations, and the variability at a fixed local time. (The JPL data are provided on the UT hour. The "local time hour" is the rounded average of the local times at the two ionospheric intersection points.)

Note: The variability is a convolved function of the electron density along the lines of sight to all satellites observed at a given time. It is greater than that of the TEC measured vertically at the station. The vertical TECs are best represented by the lower values at each time.

The right-hand panel of *Figure A-1* shows immediately that there is no unique relation between the two sets of slant TEC, even allowing for random errors. There appear to be three different relations between the two sets of observations at values of ~40 TECU (i.e., the TIDB values of TEC have three peaks when the TID2 TEC is 40 TECU.).

Figure A-2 shows the discrepancy between the TID2 and TIDB values of TEC versus the TID2 TEC (on the left), and the diurnal variations of the average and RMS discrepancies between corresponding values of TEC (on the right).
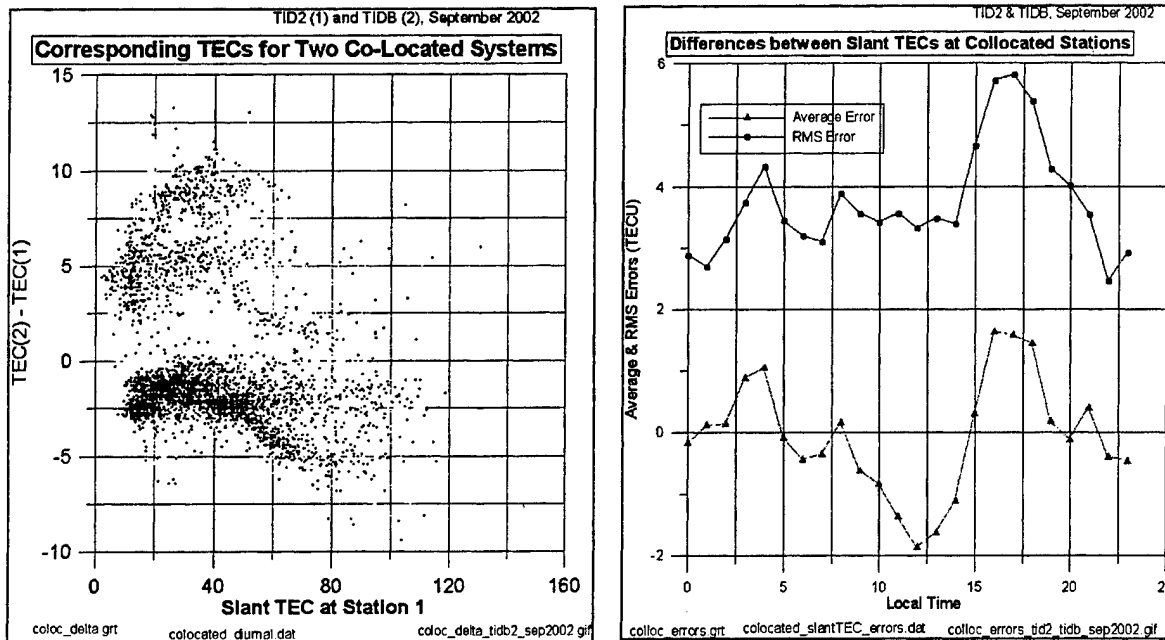
Figure A-2: Discrepancies Between TID2 and TIDB Values of Slant TEC, Sep 2002

The left-hand plot in *Figure A-2* basically provides a vertical expansion of the discrepancy between corresponding values of TEC that can be seen in the right-hand panel of *Figure A-1*.

The right-hand plot in *Figure A-2* shows the diurnal variation of the discrepancies, in terms of the average and RMS values. The averages at each hour themselves obviously have a 24-hour average of near zero, which agrees with the -0.03 TECU average given above. However, the plot shows that the values swing from -2 TECU at 12LT, up to +2 TECU near sunset. The RMS discrepancies have a diurnal average of 3.80 TECU (given earlier), with the highest values reaching ~6 TECU around sunset.

The grouping of the discrepancies into several bins (left-hand side of *Figure A-2*) suggests that the discrepancies might be a function of the local time or time (hour) of the month (i.e., UT hours since 00UT on day 1 of the month). The latter would correspond to a change in the calibrations during the month. The former might suggest a temperature effect, but the identification of the real cause would be an engineering responsibility.

Figure A-3 shows the percentage discrepancies between corresponding values of TEC as a function of time of month (on the left) and as a function of local time (on the right).
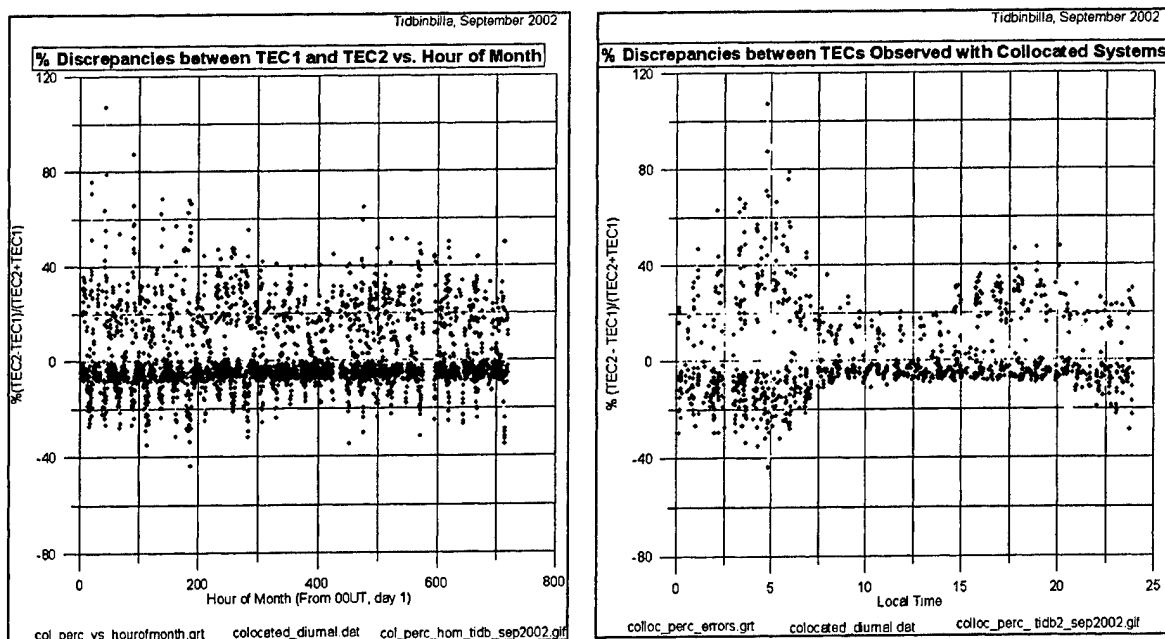
Figure A-3: Percent Discrepancy in TEC vs. Time of Month, and Local Time, TIDB, Sep 2002.

The left-hand panel does not reveal any sudden changes in the discrepancies at particular times of the month, so the discrepancies cannot be attributed to changes in the calibrations. The right-hand panel shows that percentage discrepancies are largest between 00 and 08LT, with a sub maximum between about 15 and 20 UT. The two peaks correspond to the peaks in the RMS errors that are given in *Figure A-2*.

The periodicity in the left-hand plot corresponds to the diurnal variation of the discrepancies shown in the right-hand plot. (This periodicity is clearer in the Madrid plots - q.v.) [*q.v.* (Latin, *quod vide*). Which see.]

Goldstone

Table A-3 shows the LSF straight line results for Goldstone September 2002.

Table A-3: Statistics of LSF Straight Line, Goldstone, September 2002.

Parameter	Value
Sample size (month)	3485
Slope of LSF line	0.98
Intercept of LSF line	-0.72
Average TEC1	47.40
Average TEC2	45.77
Correlation coefficient	0.997
Weighted diurnal average	-1.63
Weighted RMS discrepancy	2.66

The LSF line relating the two TECs is

$$GOLD = 0.981 GOL2 - 0.724,$$

with a sample size of 3845 and a correlation coefficient of 0.997. (This correlation coefficient can be compared with the 0.984 found for Tidbinbilla. The difference appears to be significant.)

The GOLD results (TEC2) are 1.63 TECU lower than the GOL2 (TEC1, the reference) values.

The weighted diurnal RMS error of 2.66 TECU is more representative of the discrepancies. Unlike Tidbinbilla, the positive and negative discrepancies do not cancel significantly in the average.

Figure A-4 show the diurnal variation of the GOL2 values of TEC (on the left), and the GOLD value of TEC versus the GOL2 value (on the right).
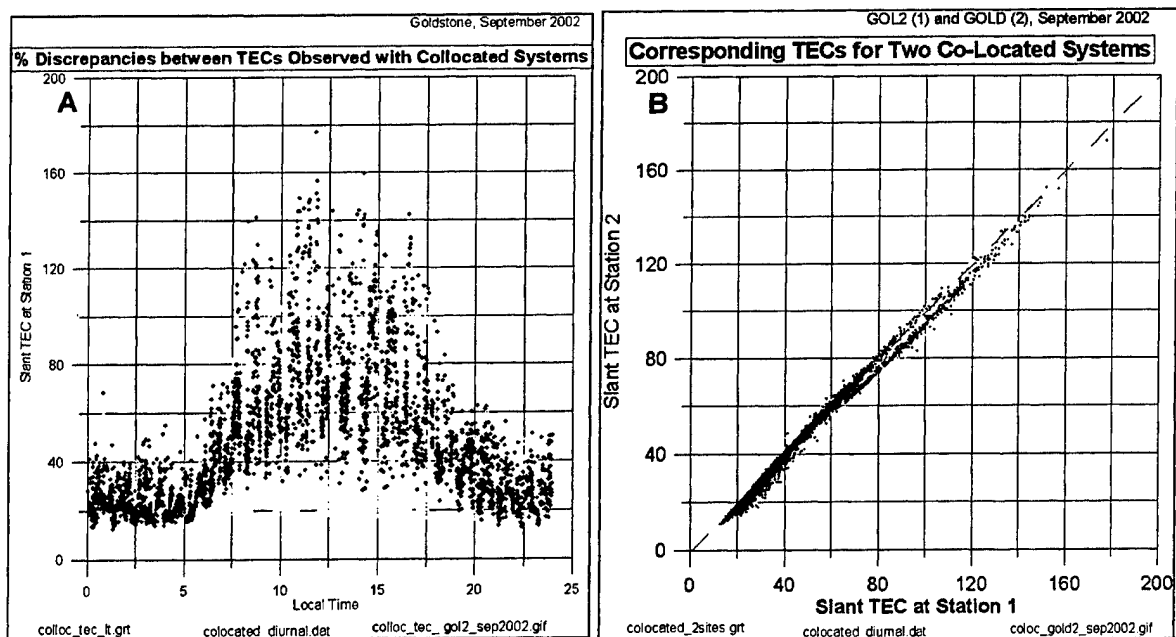
Figure A-4: Slant TECs for (A) GOL2, and for (B) GOLD Versus GOL2.

The right-hand panel of *Figure A-4* shows that there is no unique relation between the two sets of slant TEC between ~60 and ~120 TECU.

Figure A-5 shows the discrepancy between the GOL2 and GOLD values of TEC versus the GOL2 TEC (on the left), and the diurnal variations of the average and RMS discrepancies between corresponding values of TEC (on the right).
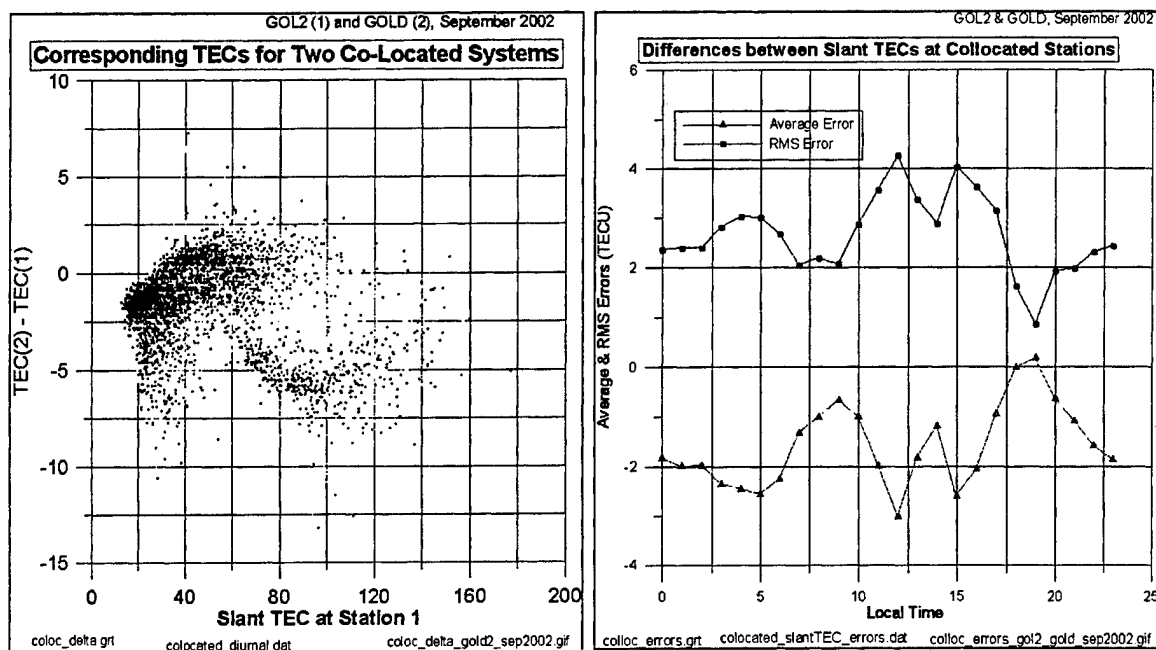
Figure A-5: Discrepancies Between GOL2 and GOLD Values of Slant TEC, Sep 2002

The left-hand plot in *Figure A-5* basically provides a vertical expansion of the discrepancy between corresponding values of TEC that can be seen in the right-hand panel of *Figure A-4*. There is a suggestion of a systematic increase in the discrepancy from about - 2 TECU to about 2 TECU as the TEC increases from 20 to 60 TECU. (The same trend is seen in the Madrid data - q.v.)

The right-hand plot in *Figure A-5* shows the diurnal variation of the discrepancies, in terms of the average and RMS values. The averages at each hour themselves have a 24-hour average of ~2 TECU, which agrees with the -1.63 TECU average given above. The RMS discrepancies have a diurnal average of 2.66 TECU (given earlier), with the highest values reaching ~4 TECU in the middle of the day.

Figure A-6 shows the percentage discrepancies between corresponding values of TEC as a function of time of month (on the left) and as a function of local time (on the right).
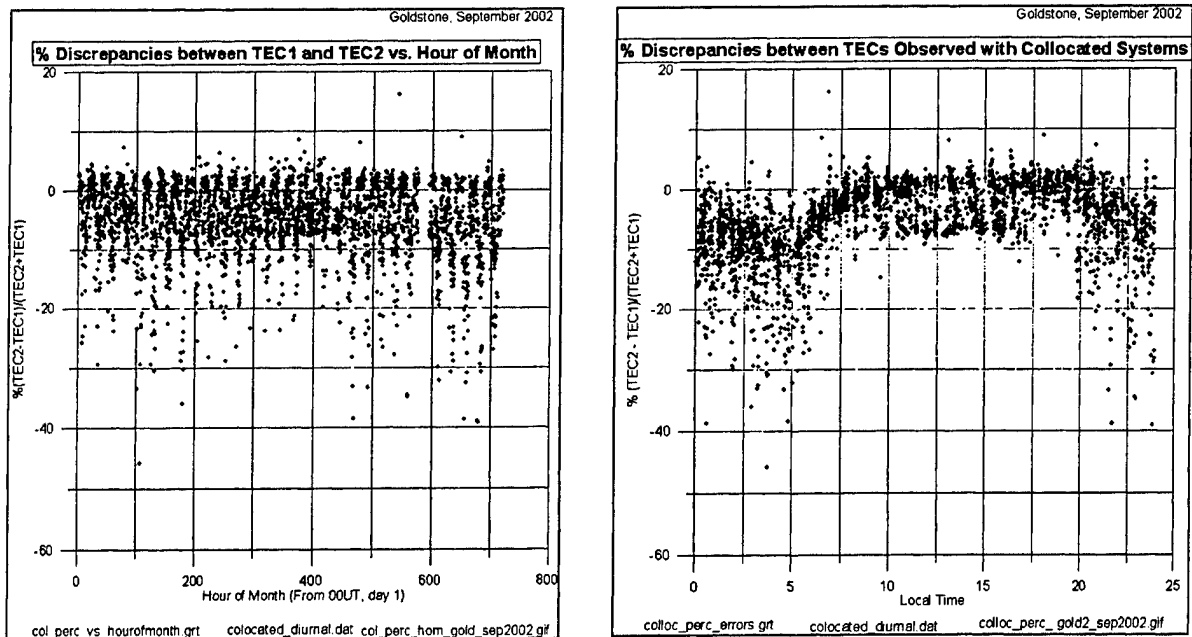
23

Figure A-6: Percent Discrepancy in TEC vs. Time of Month, & Local Time, GOLD, Sep 2002

As with Tidbinbilla, the left-hand panel does not reveal any sudden changes in the (percentage) discrepancies at particular times of the month, so the discrepancies cannot be attributed to changes in the calibrations. However, the right-hand panel shows that there is a diurnal variation in the discrepancies, with an amplitude of +/–5%. Some of the discrepancies are large and negative at night, but they correspond to only ~1 TECU.

Madrid

Table A-4 shows the LSF straight line results for Madrid, September 2002.

Table A-4: Statistics of LSF Straight Line, Madrid, September 2002.

Parameter	Value
Sample size (month)	3176
Slope of LSF line	1.01
Intercept of LSF line	-1.09
Average TEC1	46.74
Average TEC2	46.02
Correlation coefficient	0.996
Weighted diurnal average	-0.70
Weighted RMS discrepancy	1.92

The LSF line relating the two TECs is

MADR = 1.008 MAD2 -1.087,

with a sample size of 316 and a correlation coefficient of 0.996.

The MADR results (TEC2) are 0.714 TECU lower than the MAD2 (TEC1 - reference) values.

The weighted diurnal RMS error of 1.92 TECU is more representative of the discrepancies, since positive and negative discrepancies cancel in the average.

Figure A-7 show the diurnal variation of the MAD2 values of TEC (on the left), and the MADR value of TEC versus the MAD2 value (on the right).
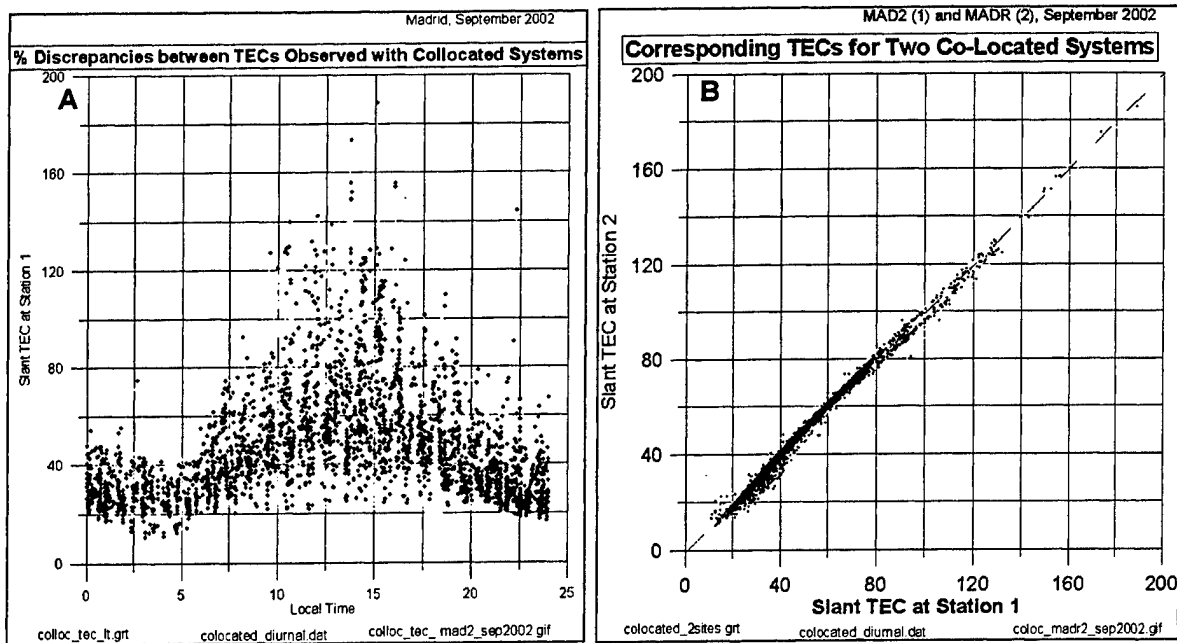
Figure A-7: Slant TECs for (A) MAD2, and for (B) MADR Versus MAD2.

The right-hand panel of *Figure A-7* shows that there is no unique relation between the two sets of slant TEC, although the spread is not as large as for Tidbinbilla (*Figure A-1*). In fact, the spread is about the same as for Goldstone (*Figure A-4*).

Figure A-8 shows the discrepancy between the MAD2 and MADR values of TEC versus the MAD2 TEC (on the left), and the diurnal variations of the average and RMS discrepancies between corresponding values of TEC (on the right).
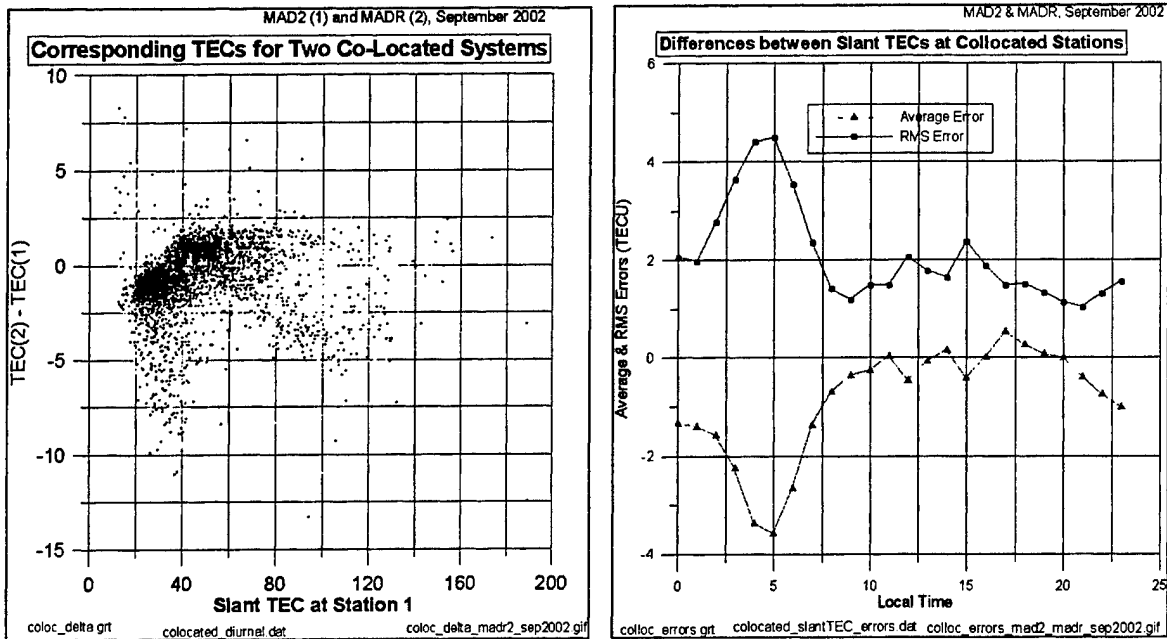
Figure A-8: Discrepancies Between MAD2 and MADR Values of Slant TEC, Sep 2002

The left-hand plot in *Figure A-8* basically provides a vertical expansion of the discrepancy between corresponding values of TEC that can be seen in the right-hand panel of *Figure A-7*.

The right-hand plot in *Figure A-8* shows the diurnal variation of the discrepancies, in terms of the average and RMS values. The averages at each hour are near zero during the day, but reach about -4 TECU just before dawn. The RMS discrepancies have a diurnal average of 1.92 TECU (given earlier), but rise to ~4 TECU just before dawn.

The large RMS error at 05 LT, i.e., 4.4 TECU, is mostly due to the large average error of -3.6 TECU. The contribution of random errors is much less. The daytime values suggest a random error of about 0.4 TECU.

Figure A-9 shows the percentage discrepancies between corresponding values of TEC as a function of time of month (on the left) and as a function of local time (on the right).
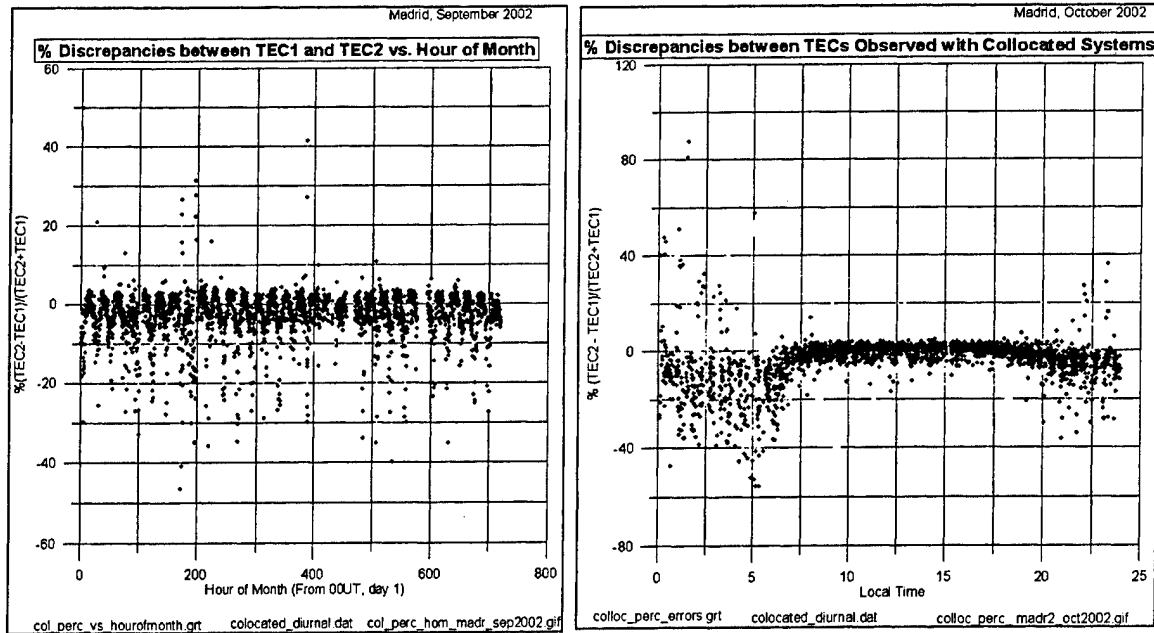
Figure A-9: Percent Discrepancy in TEC vs. Time of Month, & Local Time, MADR, Sep 2002

The left-hand panel does not reveal any sudden changes in the discrepancies at particular times of the month, so the discrepancies cannot be attributed to changes in the calibrations. However, the right-hand panel shows that percentage discrepancies are largest between 00 and 08LT. This peak corresponds to the peak in the RMS errors that are given in *Figure A-8*.

The periodicity in the left-hand plot is a manifestation of the diurnal variation of the discrepancy, which ranges between about +/- 5 TECU.

Discussion

The following figures, *Figure A-10*, *Figure A-11* and *Figure A-12*, present the 18 plots already shown, but now they are grouped by type, rather than by station. This facilitates the comparisons of results for different stations.

A perusal of the plots shows that the Madrid and Goldstone plots are similar in many respects, but differ from the Tidbinbilla plots. See, for example, the left-hand panels of *Figure A-11* and both panels in *Figure A-12*.

For summary results, the most useful comparison is of the plots of the average and RMS errors vs. local time, which are given on the right in *Figure A-11*. Summarizing these curves further, we get the weighted diurnal average values shown in *Table A-5*

Table A-5: Diurnal Averages of the Average and RMS Discrepancies at Each LT Hour.

	Weighted Average	Weighted RMS
Tidbinbilla	-0.03	3.80
Goldstone	-1.63	2.66
Madrid	-0.70	1.92

Summarizing these results still further, we can say that the discrepancies between the TECs observed by collocated JPL systems are about 2 to 4 TECU. In the absence of further information, we attribute the half the error to each system, i.e., the measurement errors are 1 to 2 TECU.

Since we have no idea of whether an isolated system is a "good", "poor" or "bad" system, we need to set the likely measurement error for such a station to the upper limit, which is +/-2 TECU.

Even this figure is probably over-optimistic, since one advantage of collocated systems is that any large differences in observed TECs would be followed by an investigation of the cause, and correction of the problem. This is not possible for isolated systems.
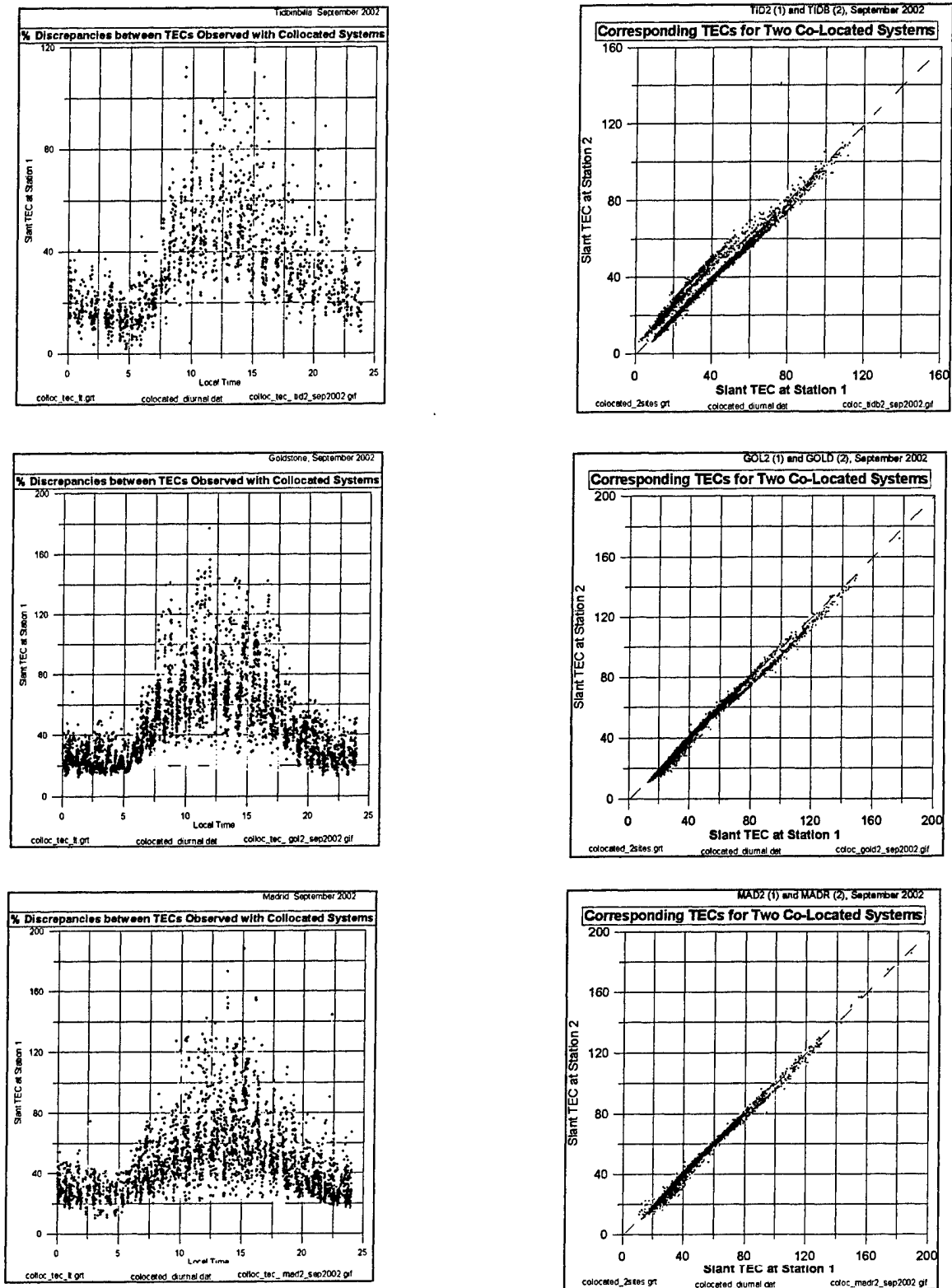
Figure A-10: Slant TECs for the Reference Station (left), &Corresponding TEC values
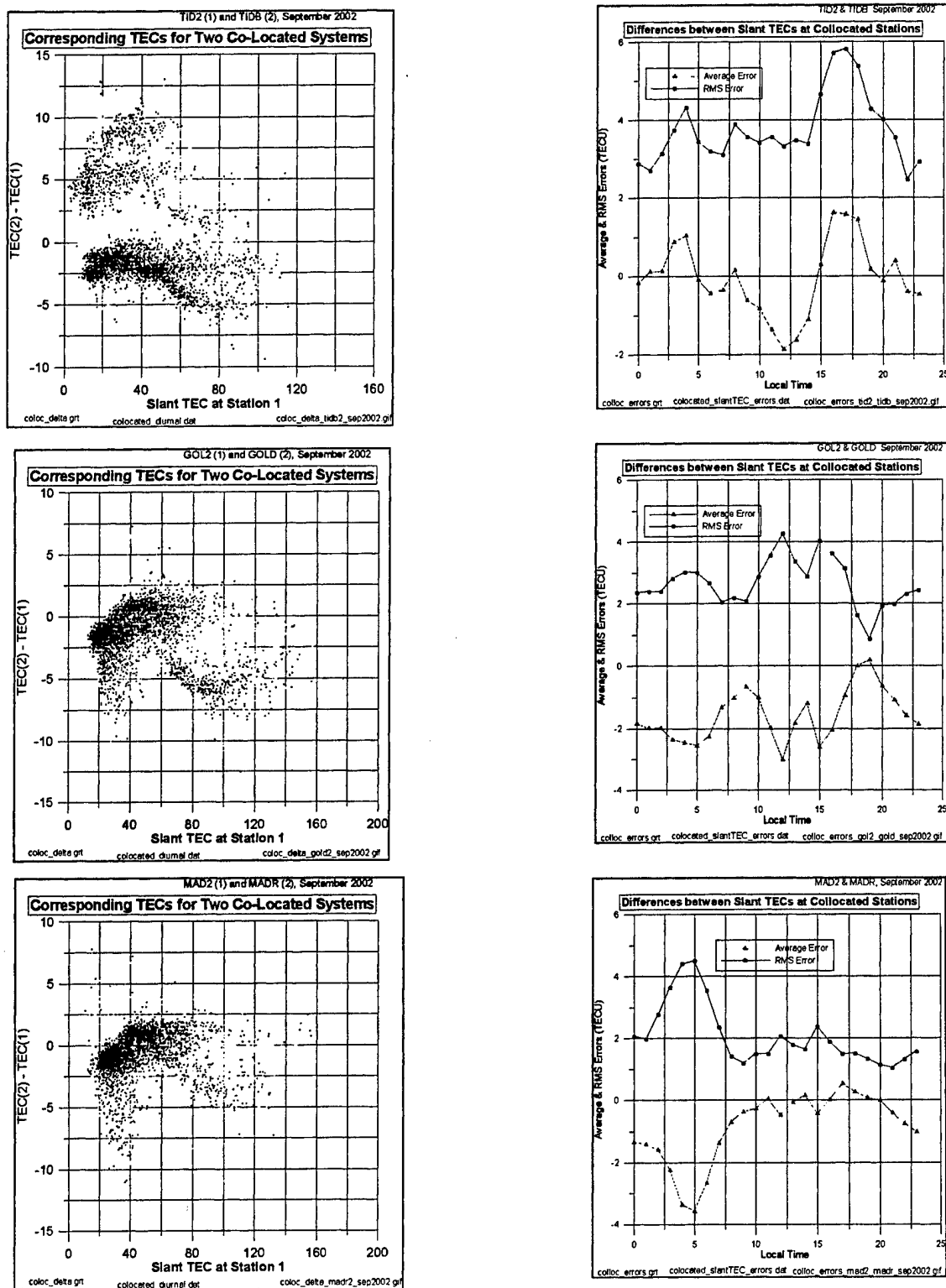
Figure A-11: Discrepancies Between Simultaneous Values of Slant TEC, Sep 2002

Figure A-12:
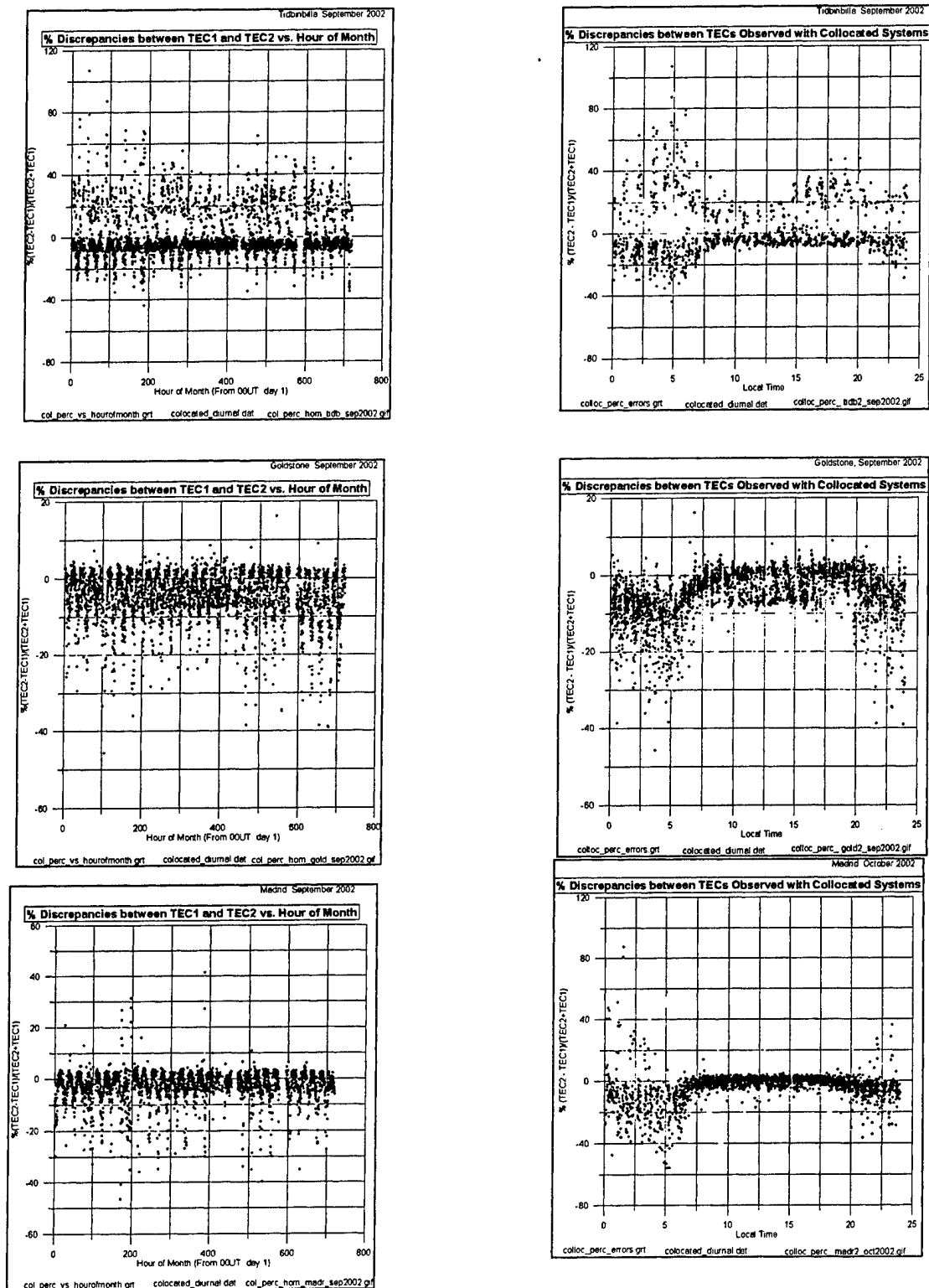

Figure A-13: Percent discrepancy in TEC vs. time of month, and local time, Sep 2002.

<div align="center">**APPENDIX B**</div>

Validity of the PRISM Sub-Peak Profile

<div align="center">February2003</div>

Summary

The procedures adopted to compare sub-peak or bottomside N(h) profiles generated by PRISM in its RTA mode (when it is supplied with observations of foF2 and hmF2) with those processed by ARTIST from digital ionograms have been described in an earlier report (*Procedures for Validating the PRISM Profile - profile_comparison_method.fm*).

This report presents the results of those comparisons. The comparisons have been made for one low-latitude station (Jicamarca) and one mid-latitude station (Vandenberg), for the first half of 2002. These stations and epochs were chosen to match the availability and reliability of automatically scaled ionograms and deduced true-height profiles. The data for Wallops Island, for example, failed too many of the quality control tests to be useful.

Several error metrics have been calculated, but the one mainly used here is the **half-thickness ymF2**. This is the vertical distance between hmF2 and the height at which the electron density has fallen to half its peak value (or the plasma frequency has fallen to 0.707 of foF2).

Note: The parameter ymF2 used here is the thickness of the F2 layer at an electron density equal to half the maximum density of the F2 layer. The same term is also used elsewhere for the thickness at a plasma frequency equal to 0.5foF2. These are not the same thing.

It has been found that

1. The distribution at each hour of the values of ymF2 is much smaller for the PRISM values than for the ARTIST values. Assuming that the width of the ARTIST distribution is due to the day-to-day variability of the physical drivers (i.e., the F2 weather), and not ARTIST analysis errors, it follows that PRISM does not provide any weather content in its calculated profiles.

2. The diurnal variation of the PRISM half-thickness tracks that of the ARTIST values reasonably well during some months, but PRISM often has a pathological behavior during the day.

3. The occurrence rate for pathological profiles is different for different stations and months. It reaches 100% for some months, such as January, February and March 2000. When the pathological cases are ignored, the average RMS error for any remaining cases is typically ~20%.

4. Pathological profiles have been found for three seasons near solar maximum for Jicamarca, and for April at the mid-latitude station Vandenberg.

5. For restricted times, the values of ymF2 are highly correlated with hmF2, and would provide a method for introducing weather effects into the PRISM's F2-layer thickness (and method of setting up the sub-peak profile).

34

The PRISM diurnal variations are tight enough to suggest that the differences from the ARTIST values (the correct results) result directly from PRISM's physical model, and not from any coding error in the extraction of the profiles from the PRISM databases. The fact that the diurnal variations of ymF2 for January, February and March 2000 correspond to the pathological results for the other months may provide some insight as to where we should start looking to determine the source of the pathologically high values of ymF2.

Navigating this Report

Because of the multi-color plots, the PRISM profile reports are designed for online reading using Acrobat. They are prepared in FrameMaker, and converted to PDF format. Blue text indicates an active link. This includes the cross-references to the figures.

The major sections in this report are

- *Summary*

- *Navigating this Report*

- *Jicamarca Results, June 2002*

- *Vandenberg, April 2002*

- *Incorporating "Weather" into the PRISM Profile*

- *Jicamarca, July 2002*

- *Jicamarca, June 2002*

- *Vandenberg, April 2002*

- *Implications of PRISM's Pathological Profiles*

- *Implications of PRISM's Pathological Profiles*

Jicamarca, July 2002

Jicamarca data has been analyzed for June and July, 2002. The July results are presented first, since they provide a good example of the pathological behavior of PRISM during the day.

Figure B-1 sets the scene, showing how the peak height of the F2 layer changes throughout the day. The peak lies at ~300 km at night, and ~375 km during the day. The high values of hmF2 at ~1900LT are associated with the reversal of the electric field and therefore of the ExB drift. In its RTA mode, PRISM matches the observed value of hmF2 (and foF2).
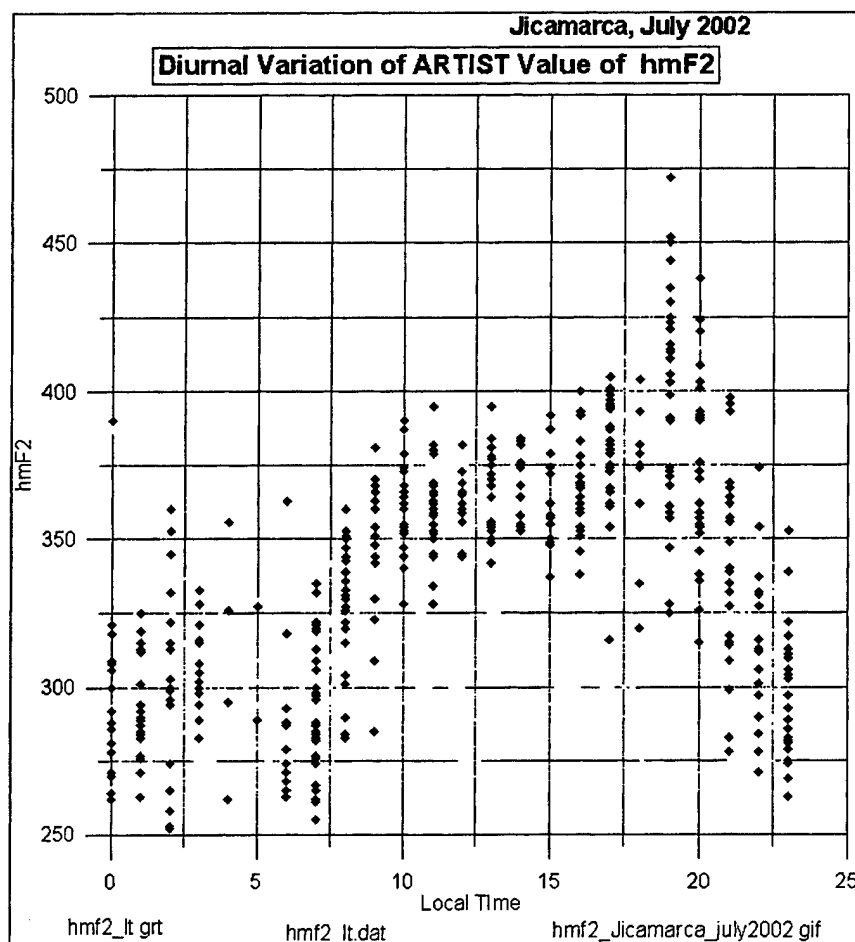

Figure B-1: Diurnal variation of ARTIST value of hmF2, Jicamarca July 2002.

Figure B-2 shows the local time variation of the thickness of the F2 layer, ymF2, as measured at 0.5NmF2, for both ARTIST (blue) and PRISM (red).
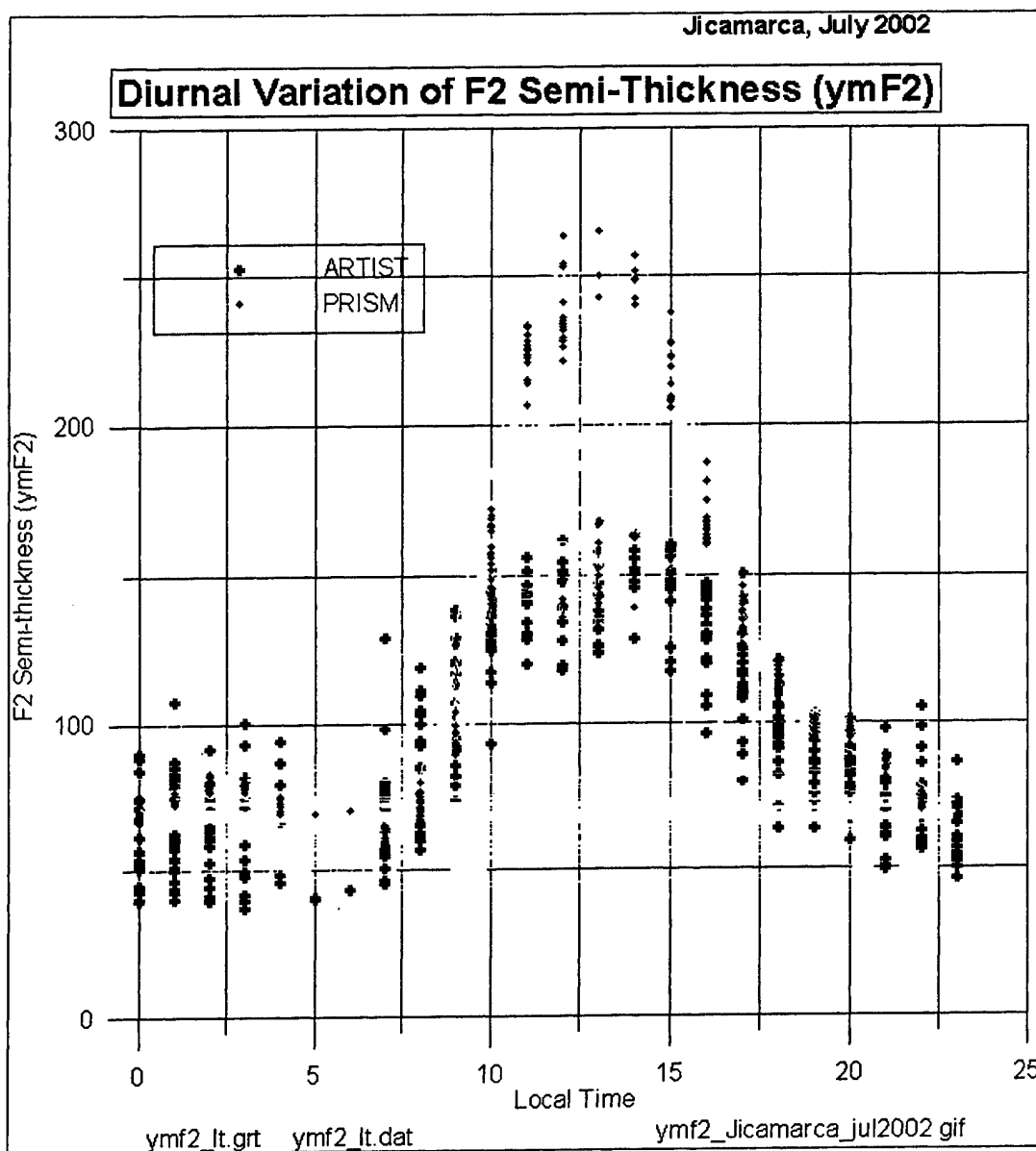
Figure B-2: Variation of PRISM & ARTIST Values of ymF2, Jicamarca, July 2002.

In general, the PRISM values of ymF2(red) track the observed diurnal variation of the observed (ARTIST) values (blue). The details of the discrepancies are discussed in the section *Validity of PRISM's Values of ymF2 (Jicamarca)*. Our first concern is with the cluster of values that lie above 200 km during the day, which are clearly pathological.

Table B-1 shows that the percentage occurrence of these pathological values (defined by ymF2 > 200 km) reaches 100% at 14 LT. The problem is confined to the daylight hours. As described in the section *Implications of PRISM's Pathological Profiles*, an F2

layer that is too thick will affect all products such as OpSEND (Operational Space Environment Network Display) that use the PRISM sub-peak ionosphere.

Table B-1: Local Time Variation of percentage good & bad values of ymF2 (vs. 200).

LT	N	GOOD	BAD
0	23	100.0	0
1	22	100.0	.0
2	22	100.0	.0
3	17	100.0	.0
4	7	100.0	.0
5	2	100.0	.0
6	1	100.0	.0
7	24	100.0	.0
8	28	100.0	.0
9	21	100.0	.0
10	23	91.3	**8.7**
11	19	.0	**100.0**
12	21	19.0	**81.0**
13	16	62.5	**37.5**
14	12	25.0	**75.0**
15	16	.0	**100.0**
16	18	100.0	.0
17	23	100.0	.0
18	26	100.0	.0
19	22	100.0	.0
20	25	100.0	.0
21	24	100.0	.0
22	24	100.0	.0
23	20	100.0	.0

The pathological values of ymF2 occur only from 10LT to 15LT. The exact numbers in the table are irrelevant because of the small sample sizes.

Figure B-3 shows the PRISM plasma frequency profiles, along with the corresponding ARTIST profiles, for 1300 and 1400LT on 2002/184 (3 July).
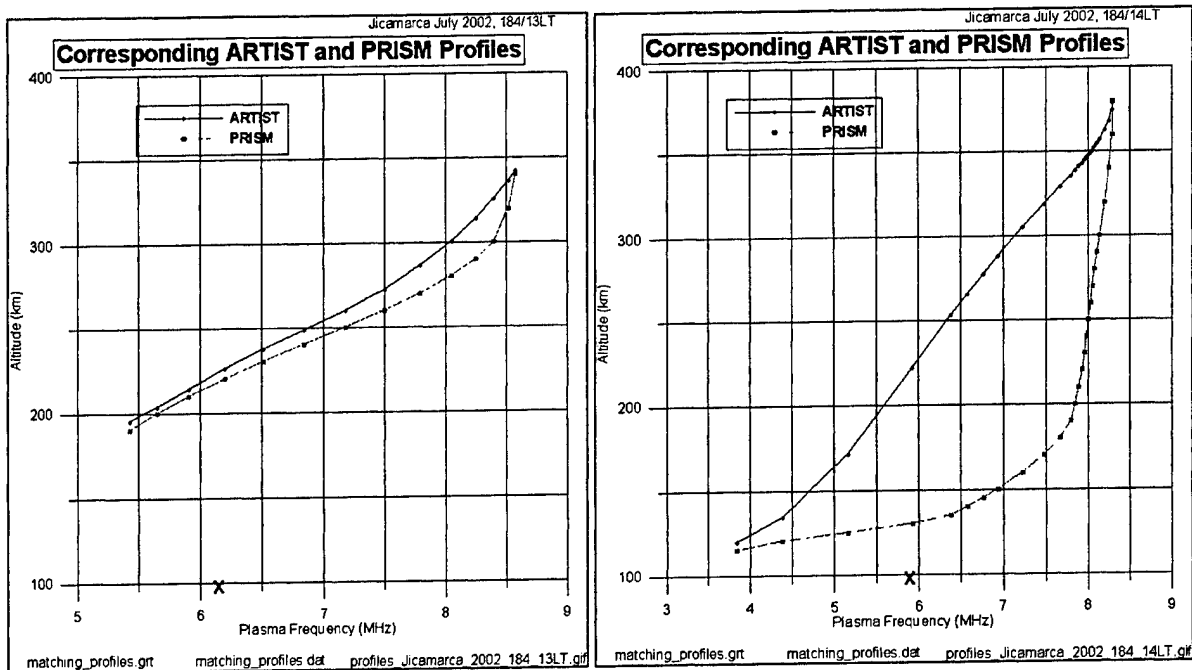
39

Figure B-3: ARTIST and PRISM Profiles for Jicamarca 184/13LT and 184/14LT.

Clearly, PRISM's F2 layer is far too broad at 1400LT. It would be expected that the PRISM profiles would be very similar at the two times, which are only one hour apart. (The **x** along the frequency axis indicates the frequency equal to 0.707 foF2.)

Given that the PRISM RTA profile is often pathological during the day, the next question is what is the cause - PRISM's CLM profile, or the RTA adjustment scheme that moves and reshapes the CLM profile. We look first at some daytime CLM profiles.

Figure B-4 shows the diurnal variation of PRISM's climatology (CLM) values of ymF2 for Jicamarca, July 2002.

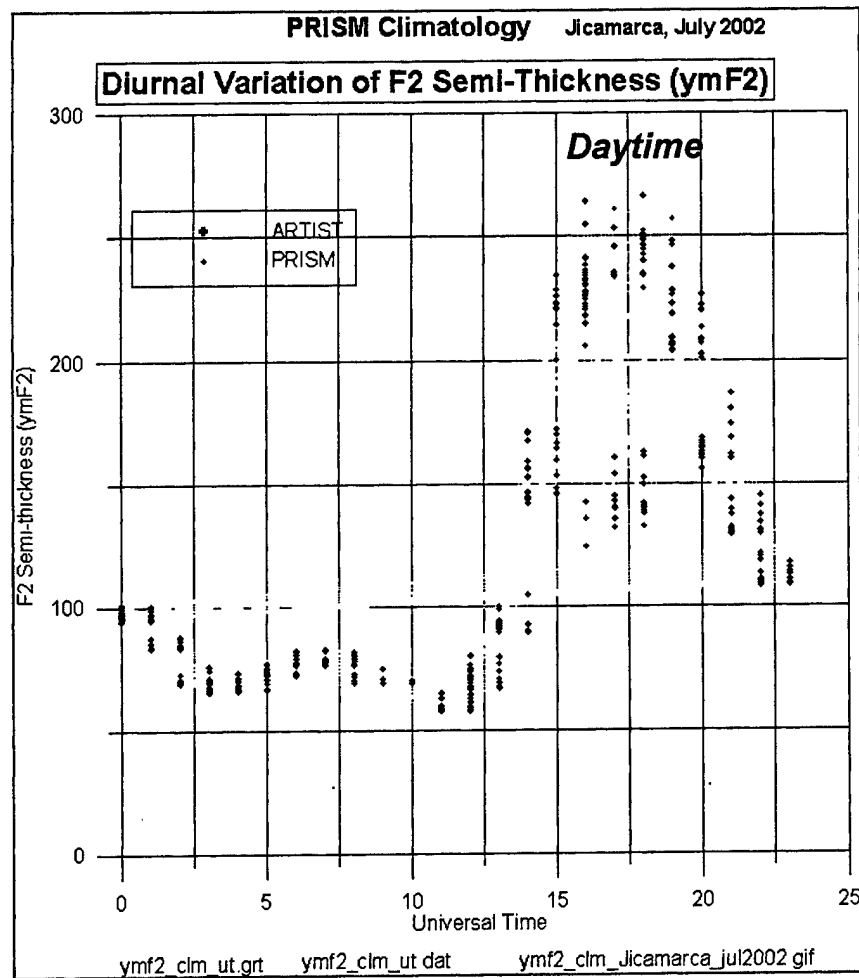**Note:** The x axis in *Figure B-4* is UT, which is LT+5.

40

Figure B-4: Diurnal Variation of PRISM Value of ymF2, Jicamarca, July 2002.

This figure suggests that PRISM's climatology daytime profile is a large part of the cause of most of PRISM's pathological values of ymF2, i.e., the values greater than 200 km.

Example PRISM CLM Profiles

Figure B-5 shows two climatology profiles for Jicamarca, July, 2002.
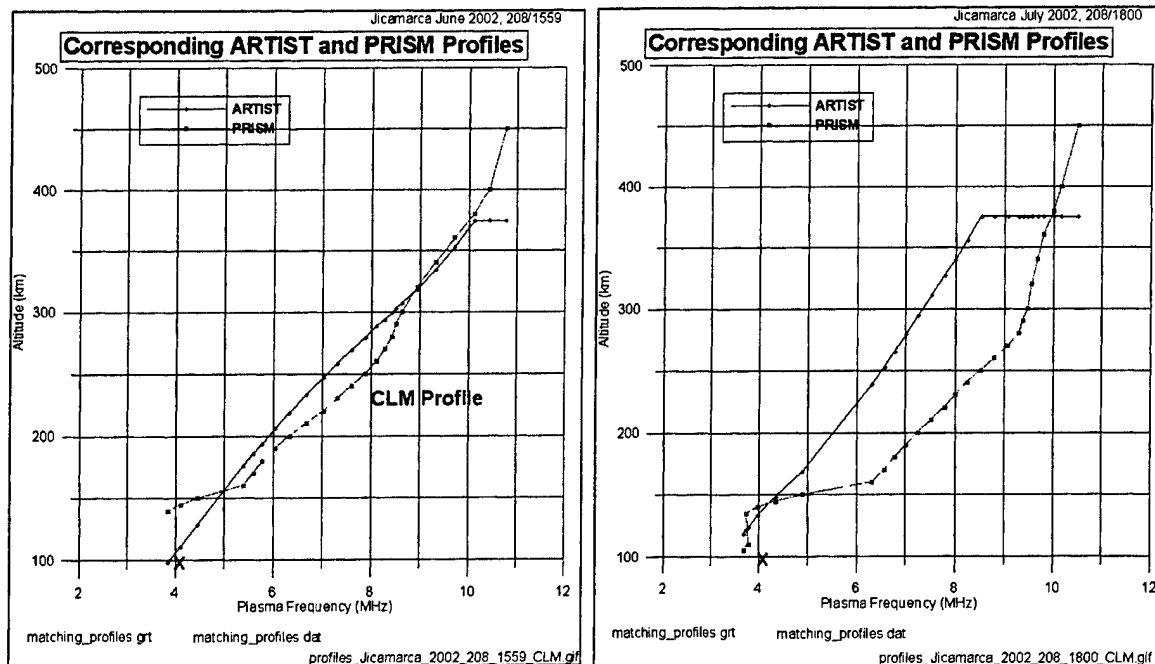
41

Figure B-5: Midday PRISM Climatology Profiles, Jicamarca, July 2002.

The profiles on the left are for 208/1559UT. Although there are differences between the ARTIST and PRISM peak parameters, the PRISM profile is a good match to the ARTIST profile. The PRISM profile on the right (208/1800) is also a good match, since it can (also) be slid to lower frequencies and heights without a large amount of distortion.

As can be seen from *Figure B-6*, the RTA profile was good for 1800UT (the plot on the right), with a semi-thickness within 10 km of the ARTIST value. However the RTA profile for the 1559UT ionogram was pathological, with a semi-thickness of 233 km.
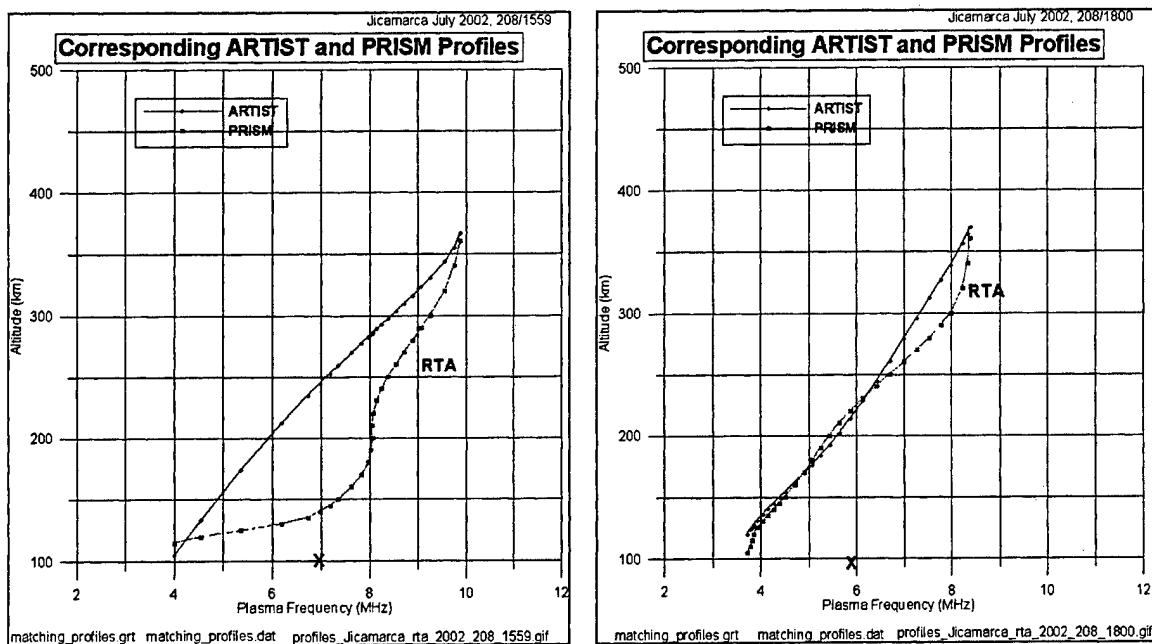
42

Figure B-6: Midday PRISM RTA Profiles, Jicamarca, July 2002.

Thus, although Figure B-4 suggests that the CLM profiles are the source of the pathological RTA profiles, the picture is not so clear cut. At least some of the problem lies in the failure of the profile-updating algorithm, even under relatively simple conditions. Much more detailed analyses will be required to isolate and remedy this problem.

Validity of PRISM's Values of ymF2 (Jicamarca)

Figure B-7 shows the diurnal variation of the average and RMS discrepancies between the ARTIST and PRISM values of ymF2, versus UT, ignoring the pathological profiles.
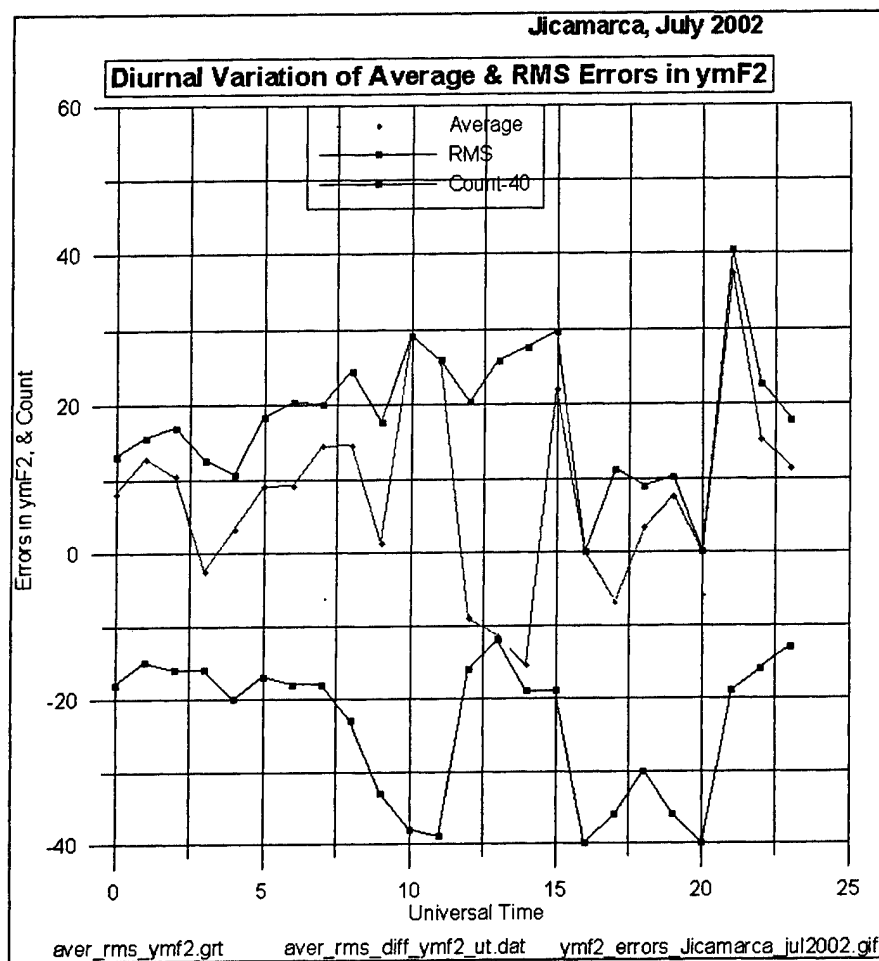

Figure B-7: Variation of the average and RMS errors in ymF2, Jicamarca, July 2002.

These curves ignore the pathological points. The average errors in ymF2 for the month (red) are ~10km, while the RMS error is ~20km. These are the characteristic errors that would propagate through to products such as OpSEND

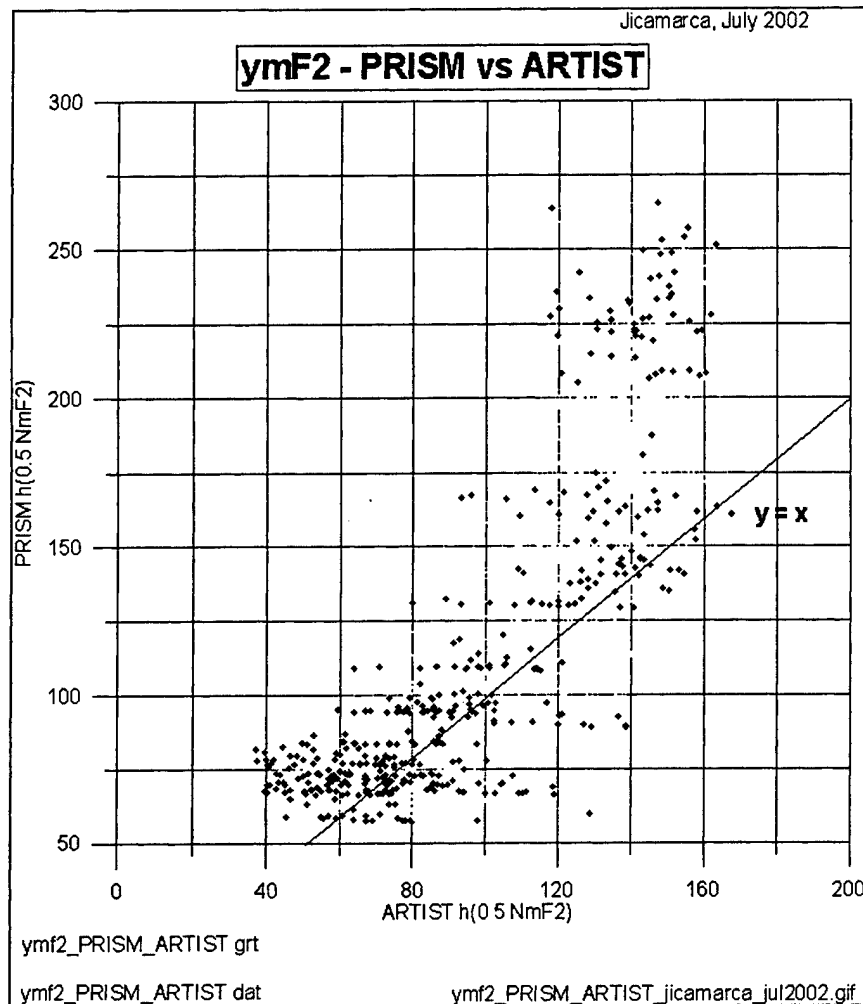*Figure B-8* shows the corresponding PRISM and ARTIST values of ymF2.

Figure B-8: Corresponding Values of ARTIST and PRISM Values of ymF2.

The y = x line is provided as a reference. PRISM tends to overestimate the higher values of ymF2, roughly 150 km vs. 135 km. The cluster at the top includes the pathological points, which are ~85km too high (225 - 140), for the center of the cluster.

The error distribution is larger in the x direction than in the y direction, corresponding to a small range in the PRISM values and a large range in the ARTIST values. The large spread in the x-direction gives rise to the large observed RMS errors. In Figure B-2, the visual equivalent is the red dots (PRISM) being more closely distributed than the ARTIST values (blue).

Physically, this corresponds to there being no day-to-day variability in the PRISM profile, whereas the ARTIST values have a spread of about +/- 30 km. In other words, there is no weather in the shape of the PRISM profiles. PRISM RTA matches the observed value of foF2, so there is weather at least in the peak parameters.

45

Jicamarca Results, June 2002

The Jicamarca results for June 2002 are very similar to those for July, so they will be presented here with little discussion. The pathological behavior of PRISM during the day is also present in this month.
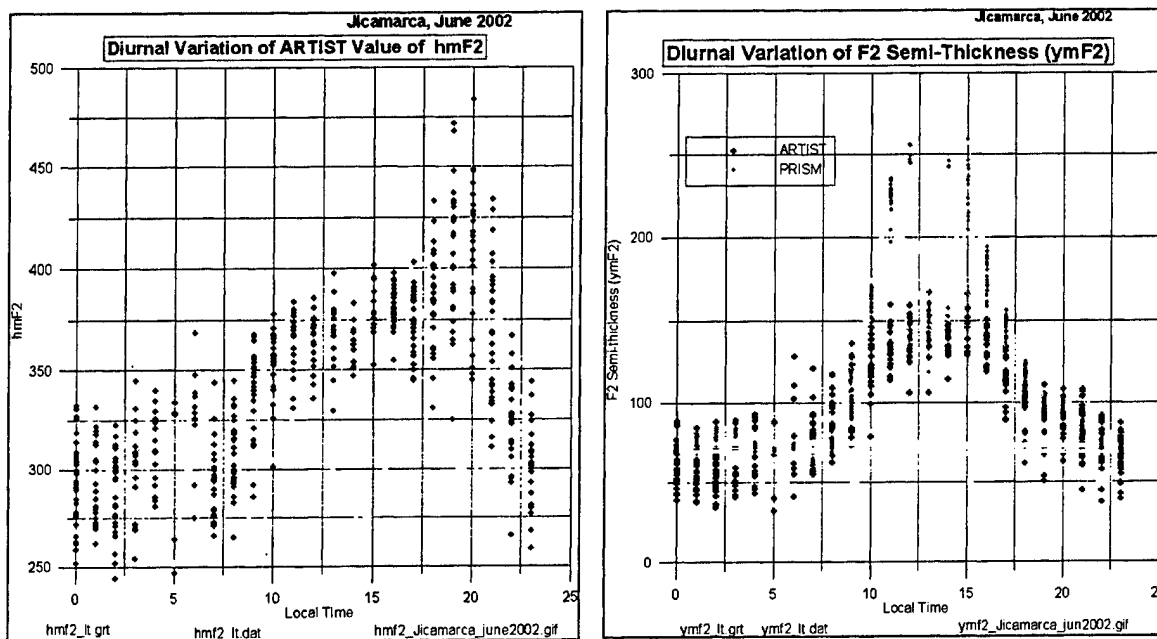

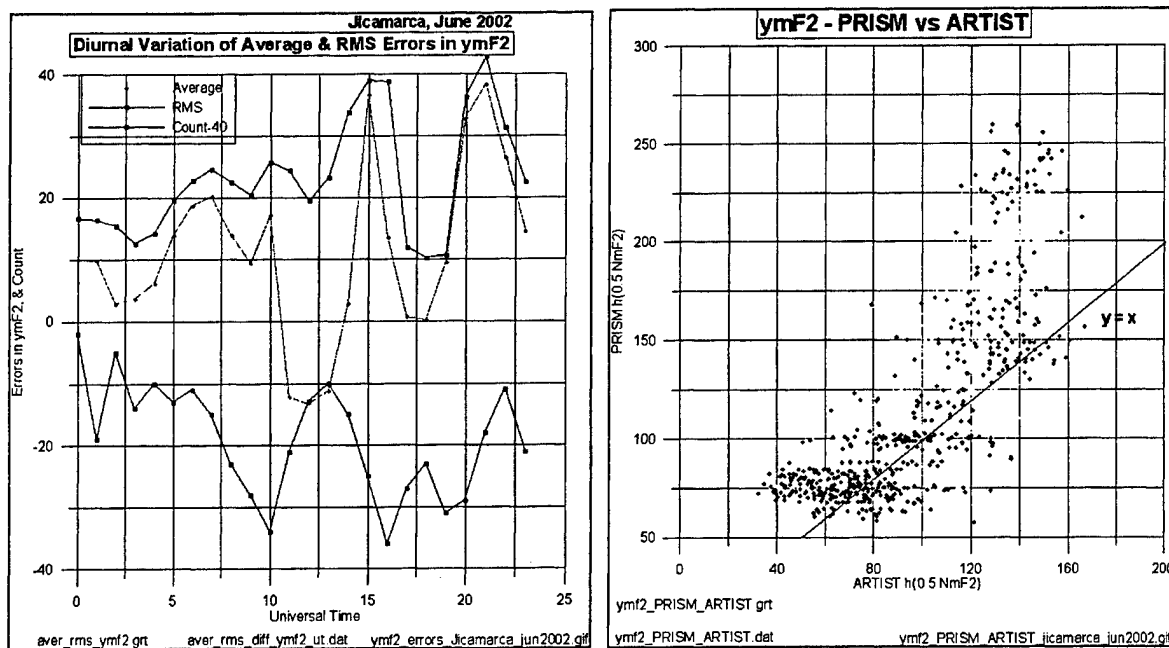*Figure B-9: Diurnal Variation of hmF2 and ymF2, Jicamarca, June 2002.*

Figure B-10: Errors in PRISM Values of ymF2, and PRISM ymF2 vs., ARTIST ymf2.

Vandenberg, April 2002

The Vandenberg (Point Arguello) results are presented here mainly to show that the pathological PRISM daytime profiles are not restricted to low latitudes. Vandenberg is at a latitude of 34.4N, and is a mid-latitude station.
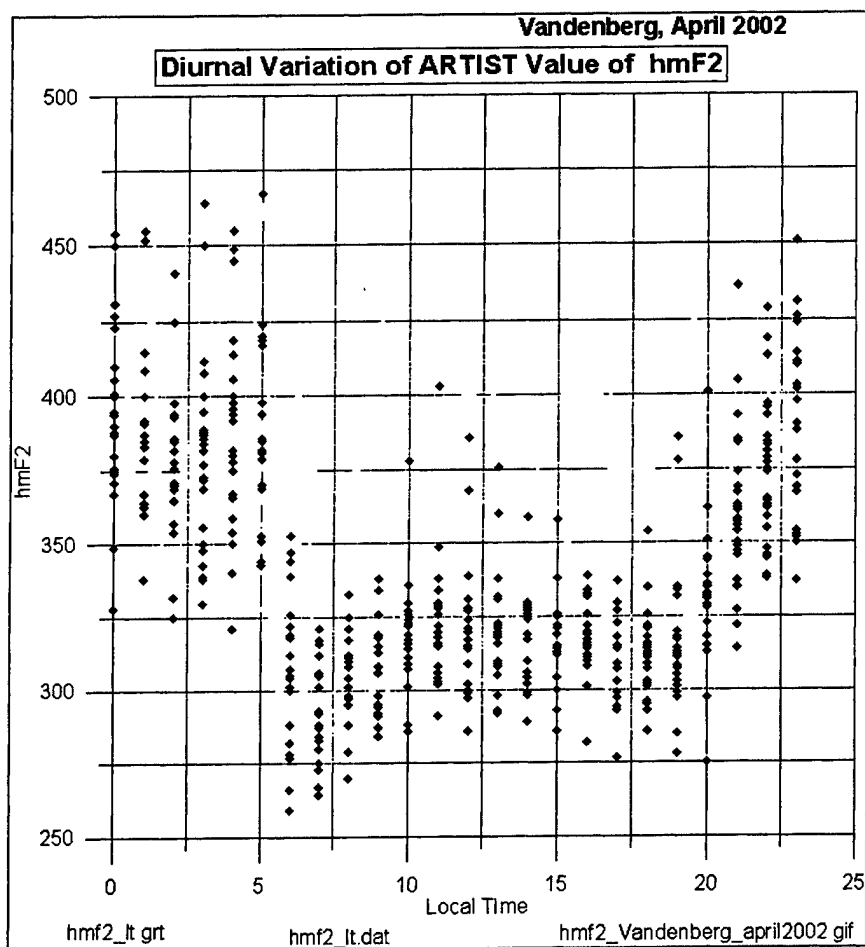
Figure B-11: Diurnal Variation of ARTIST Value of hmF2, Vandenberg, April 2002.

Comparing *Figure B-11* with the Jicamarca results in *Figure B-1* shows the very different diurnal variations for the low and mid-latitude sites. At Jicamarca, the highest values of hmF2 occur during the middle of the day, with even higher values associated with the reversal of the ExB drifts. At Vandenberg, the highest values occur at night, when they are ~60km higher than the daytime values.

Figure B-12 shows the diurnal variation of the ARTIST and PRISM values of ymF2.
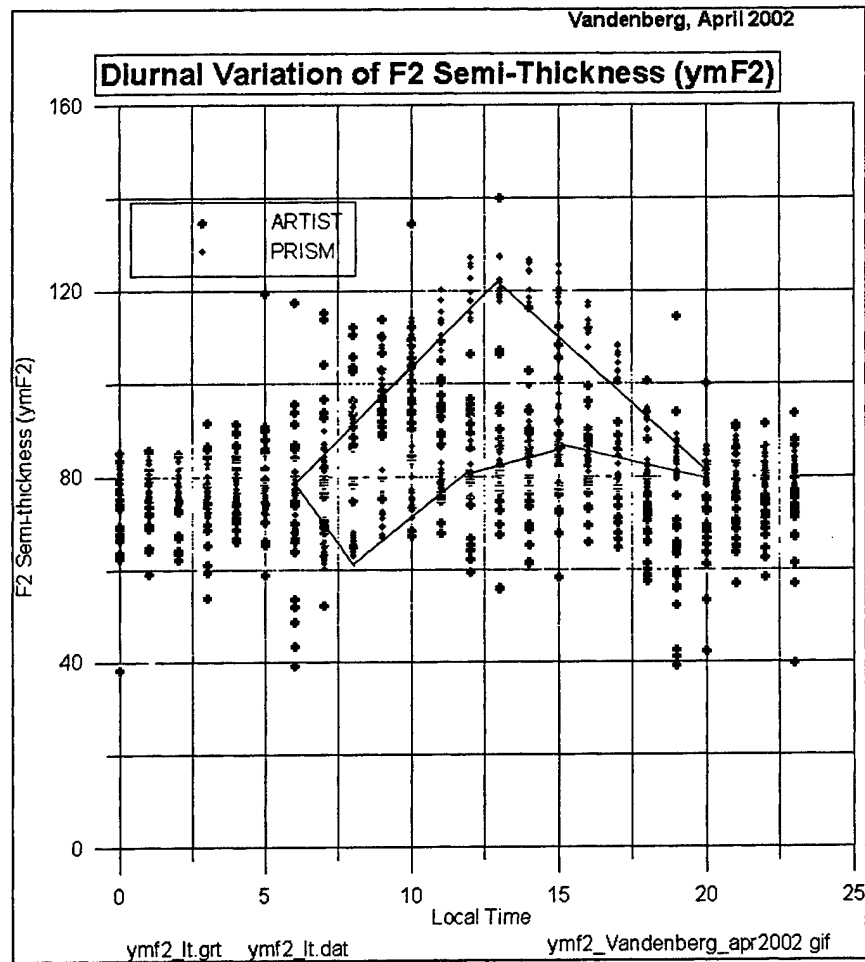
Figure B-12: Variation of PRISM & ARTIST Values of ymF2, Vandenberg, April 2002.

The PRISM distributions between 0700 and 1800LT are clearly bimodal. (The superimposed straight lines highlight this effect.) This bimodal structure was also seen for Jicamarca, but only during the day, probably because of the lower sample sizes for Jicamarca. The bimodal distribution for Vandenberg suggests that the tendency for PRISM to produce pathological profiles is not restricted to the daytime.

Figure B-13 shows the diurnal variation of the error in ymF2. The upper limit for acceptable values of ymF2 was set at 100km.

Figure B-13: Variation of Average and RMS Errors in ymF2, Vandenberg, April 2002.

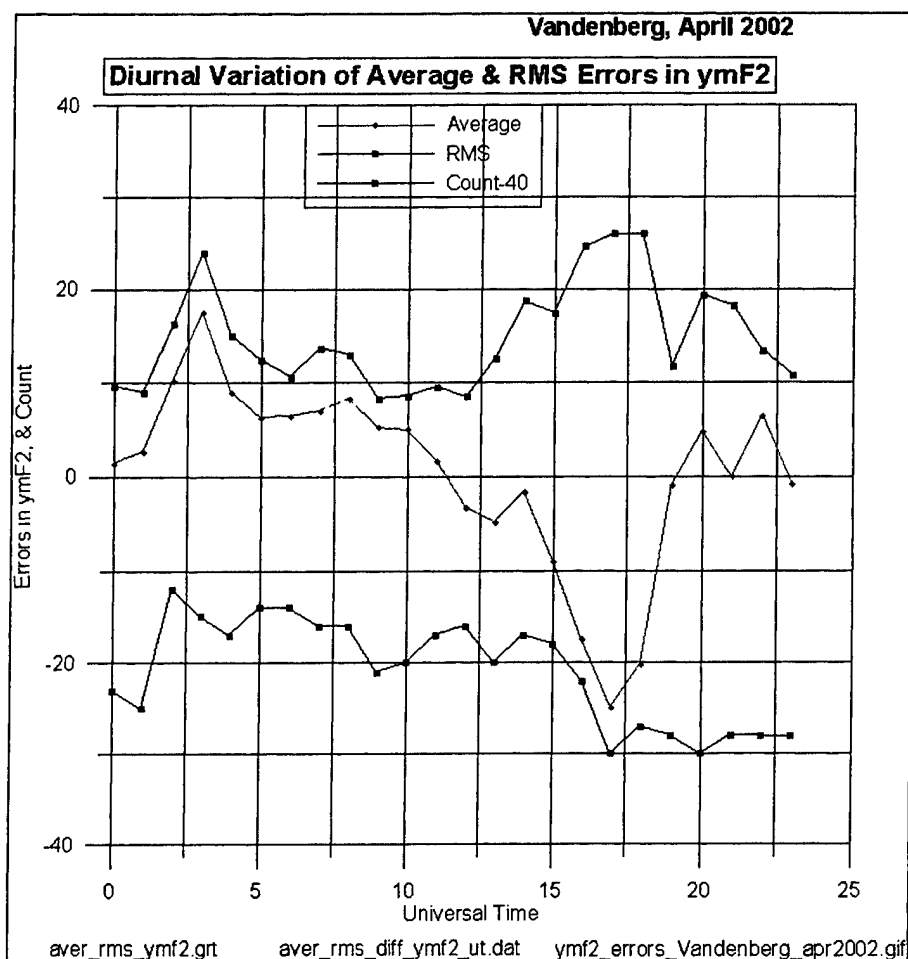The average errors are large and negative at ~1500 to 1800LT. The RMS error throughout the day is ~15km, or (15/80 = ~20%).

Incorporating "Weather" into the PRISM Profile

When working in its RTA mode, PRISM tracks the weather (day-to-day variability) of the F2 peak, since it matches the values of foF2 and hmF2 supplied to it. However, as can be seen from the plots of ymF2 vs. local time (e.g., *Figure B-2*), the day-to-day variability of the PRISM semi-thickness is much narrower than that of ARTIST (the "real" ionosphere).

The remainder of this report compares the ARTIST values of ymF2 and hmF2. If there is a relationship between them, it can be used to introduce weather into the semi-thickness of the layer.

Possible correlations have been investigated for four cases:

1. ymF2 vs. foF2

2. ymF2 versus hmF2

3. ymF2 (PRISM) vs. ymF2 (ARTIST)

4. ymF2 (PRISM) vs. foF2/foE

The data has been broken up into eight 3-hour local time bins, 00-02, 03-05, etc. Recall that all data is hourly data. Correlations have been derived for each LT bin, bins 1 through 4, all daytime bins, and all nighttime bins. Each set of data is characterized by the correlation coefficient, and the slope and intercept of the LSF straight line.

Only the second set of data (ARTIST ymF2 versus hmF2) provides any useful correlations. It is found that significant correlations between the ARTIST values of ymF2 and hmF2 exist, between midnight and noon for Jicamarca, and for post-sunrise and post-sunset for Vandenberg.

The observed correlations arise from the interplay between hmF2, ymF2 and h(0.5NmF2), which are related by hmF2 = ymF2 + h(0.5NmF2). or Jicamarca, part of the correlation may be due to the fact that the F2 layer is linear (i.e., the plasma frequency is a linear function of altitude). See, for example, *Figure B-3*.

Jicamarca, July 2002

The correlations for Jicamarca, July 2002, are shown in *Table B-2*.

Table B-2: LSF Lines for Different Pairs of Profile Parameters, Jicamarca, July 2002.

Bin		Correlation Coeffs				Slopes of LSF Line				Intercepts of LSF			
1	67	-.27	**.78**	-.03	.00	-4.19	**.51**	-.01	.00	89.	**-88**	74.	0.
2	26	-.03	**.81**	-.07	.00	-.79	**.58**	-.01	.00	68.	**-112.**	77.	0
3	53	24	**.88**	-.02	-.22	4.05	**.75**	-.01	-17.7	44.	**-144.**	66.	132
4	63	-.52	**.75**	.56	-.38	-16.2	**.66**	1.54-	28.7	276.	**-103.**	-43.	199.
5	49	-.43	.13	.04	-.33	-11.7	.12	.13	-31.9	243.	98.	180.	214
6	57	-.68	.35	.60	-.61	-16.5	.43	1.09	-20.7	274.	-30.	25.	191.
7	73	.03	.34	.52	.00	.36	.14	.30	00	88.	34.	74.	0.
8	68	.16	**.70**	.23	.00	2.21	**.26**	.14	.00	54.	**-15.**	65.	0.

```
Bins 1-4: Count, Gradient, Intercept, Correl Coeff 209    .86 -182.    .88
Day Bins: Count, Gradient, Intercept, Correl Coeff  71    .78 -152.    .81
Night Bins: Count, Gradient, Intercept, Correl Coeff 234    .30  -27.    .78
```

The numbers that have been bolded are for the correlation between ymF2 and hmF2. The last three lines are also for this correlation. This is the only combination of physical parameters that has any significance. The second column gives the sample sizes.

Figure B-14 shows the corresponding values of the ARTIST Jicamarca values of ymF2 and hmF2, for hours 00LT to 11LT, July 2002. The LSF straight line is

$$hmF2 = 0.86 \ hmF2 - 182$$

with a correlation coefficient of 0.88, which suggests that a useful relationship exists between the two parameters.
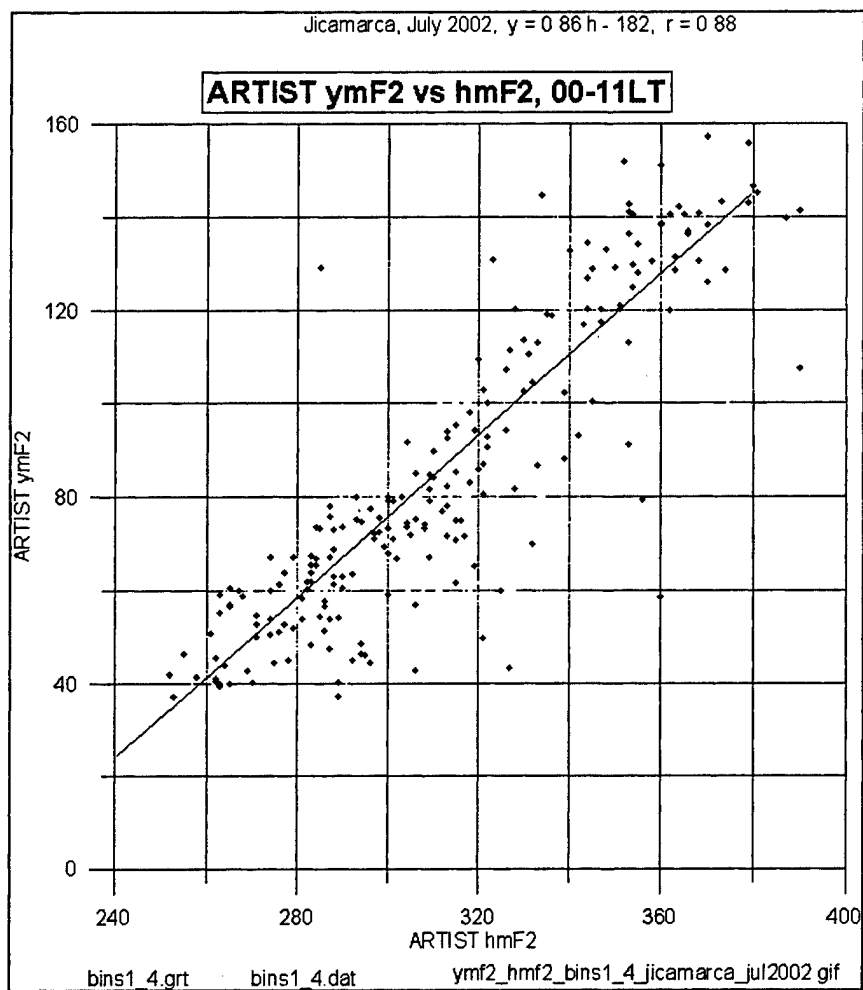
Figure B-14: Corresponding Values of ymF2 and hmF2, Jicamarca, July 2002.

However, there is no apparent relationship between ymF2 and hmF2 for 12-20LT.

A closer look at the data reveals the source of the apparent correlation between ymF2 and hmF2 in the interval 00 and 12LT. *Figure B-15* shows the individual values of the height at 0.5 NmF2, which is just hmF2 - ymF2.
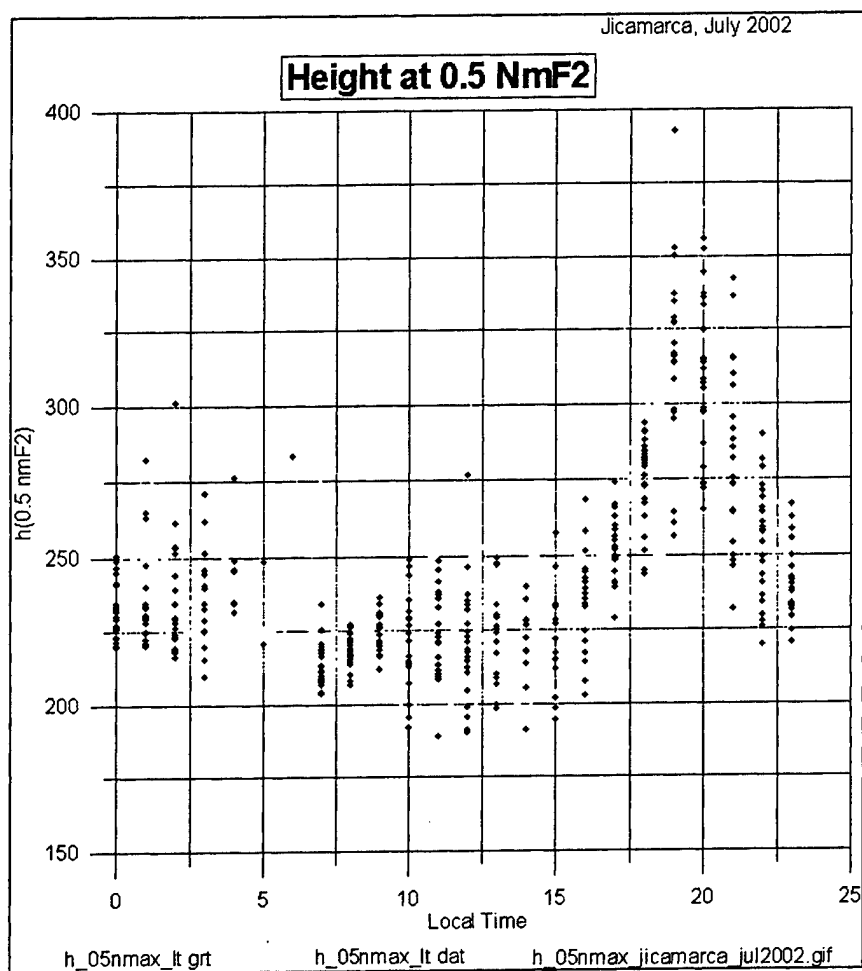
Figure B-15: Diurnal Variation of h(0.5NmF2), Jicamarca, July 2002.

The essential difference between the intervals 00-12LT and 12-00LT is that the values of h(0.5NmF2) are reasonably constant during the first interval, at ~230+/- 20 km. As can be seen from Figure B-1, hmF2 varies from 275 to 375 km during this interval, which is a range five times that of the range in h(0.5NmF2). The variation of ymF2 from 40 to 140 km (Figure B-14) is mostly the result of the variation of hmF2.

Jicamarca, June 2002

The correlations for Jicamarca, June 2002, are shown in *Table B-3*.

Table B-3: LSF lines for different pairs of profile parameters, Jicamarca, June 2002.

Bin	#	Correlation Coeffs				Slopes of LSF Line				Intercepts of LSF			
1	84	19	.88	.02	.00	3.14	.57	01	.00	40.	-105.	77	0.
2	41	-.26	.84	-.04	.00	-5 83	.59	-.01	.00	93	-113.	78.	0
3	68	.20	.80	.14	.25	1.88	64	.05	25 3	67.	-114.	65.	-1.
4	73	-.45	.83	.51	-.58	-10.5	.74	1.43	-39 1	227.	-139.	-15.	231.
5	53	-.45	.27	.20	-.44	-8 27	.25	.69	-30.8	216	49.	66.	215.
6	67	-.50	.59	57	- 38	-11.9	68	1 23	-10.4	-128	17.	164	239.
7	82	-.08	.47	.39	.00	-1.87	.22	.23	.00	110.	4	84	0
8	86	.04	.81	.41	.00	.77	.32	.20	00	67.	-31	62.	0.

```
Bins 1-4: Count, Gradient, Intercept, Correl Coeff 266    .84 -181.    .91

Day Bins: Count, Gradient, Intercept, Correl Coeff  82    .70 -132.    .77

Night Bins: Count, Gradient, Intercept, Correl Coeff 293    .32  -32.    .84
```

As with the July results, the only significant correlation is between ymF2 and hmF2. It is low for bins 5, 6 and 7, i.e., 12-20LT.

Figure B-17 shows the corresponding values of ymF2 and hmF2 for June, 2002.
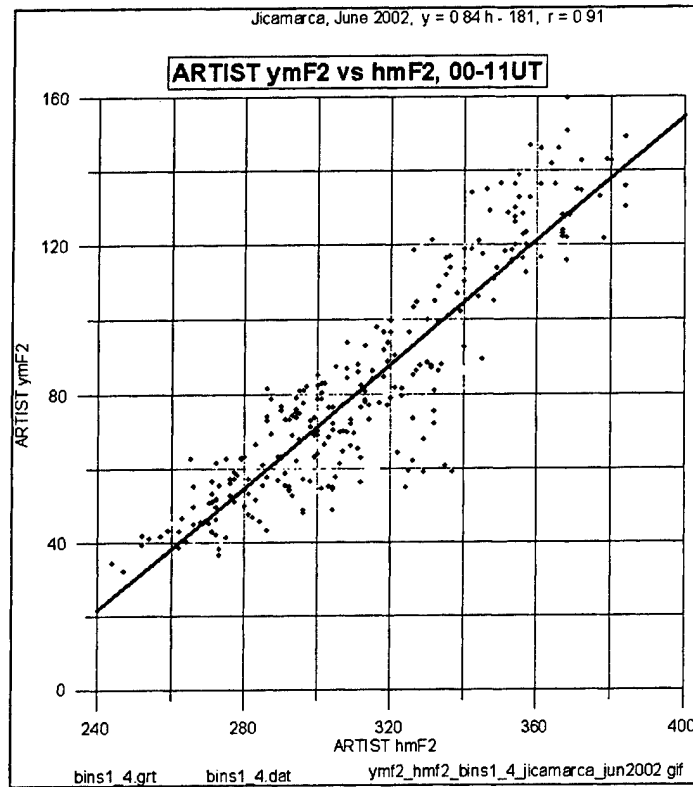
Figure B-16: Diurnal variation of h(0.5NmF2), Jicamarca, June 2002

This figure is very similar to *Figure B-14*, which gives the July results. Likewise, the h(0.5NmF2) plot of *Figure B-16*, is very similar to *Figure B-15*.
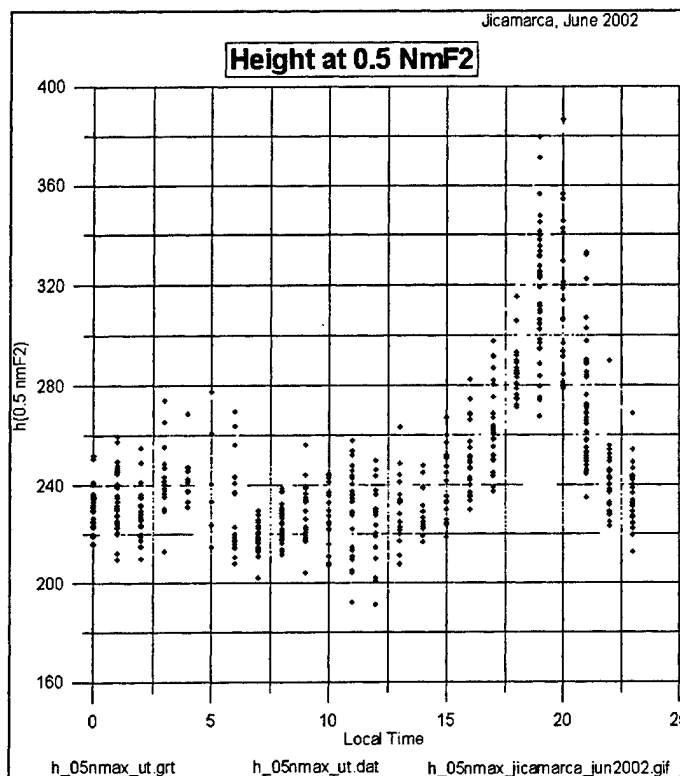
Figure B-17: Corresponding Values of ymF2 and hmF2, Jicamarca, June 2002

We can conclude from *Figure B-14* and *Figure B-17* that there is an apparent correlation between values of ymF2 and hmF2 during the midnight to noon period for both June and July, but that this correlation really follows from the fact that the height at 0.5NmF2 stays fairly constant at ~230 km during that time, while the values of hmF2 vary in almost a linear fashion, causing the values of ymF2 to follow.

"Weather" can thus be incorporated into the PRISM model of the sub-peak F2 layer simply by assimilating real-time values of foF2 and hmF2, and forcing PRISM's profile to pass through 230 km at 0.5NmF2. However, this approach is valid for only the midnight to noon period.

Vandenberg, April 2002

The Vandenberg correlation results are given in *Table B-4*.

Table B-4: LSF Lines for Different Pairs of Profile Parameters, Vandenberg, April 2002

Bin	#	Correl Coeffs				LSF Line Slopes				LSF Line Intercepts			
1	63	-.37	.54	.07	.00	-4.78	.15	.02	.00	102.	14.	77.	0
2	67	-.46	.46	.15	.00	-7.10	.14	.04	.00	118.	23.	72.	0.
3	63	.13	.74	23	-.24	1 71	63	.13	-11.6	68.	-108.	63.	118
4	61	- 56	.44	.05	-.32	-6.48	.28	.06	-13.8	161	3.	85.	133
5	62	- 64	.29	-.02	-.56	-7.34	.23	-.02	-18.2	163.	10.	104.	136.
6	68	-.51	.48	-.04	-.59	-4.11	.40	-.05	-13.4	125.	-42.	99.	127.
7	76	-.30	.79	-.10	- 20	-2.78	48	-.03	-3.04	95.	-81.	85.	84.
8	76	-.26	.57	-.14	.00	-4.04	.19	- 05	00	102.	5.	85.	0.

```
Bins 1-4: Count, Gradient, Intercept, Correl Coeff 254   -.02    89.   -.08

Day Bins: Count, Gradient, Intercept, Correl Coeff 242    .53   -82.    .58

Night Bins: Count, Gradient, Intercept, Correl Coeff 282    .14   24.    .50
```

None of the correlations in the last three lines is significant. The high correlation that was found for bins 1-4 for Jicamarca is essentially zero for Vandenberg. However, the bolded column indicates that the correlation coefficients for individual bins can in fact be quite high.

Figure B-18 shows the corresponding values of hmF2 and ymF2 for bins 1-4 (00-11LT), on the left, and bin 7 (18-20LT) on the right. It is clear that there are in fact two separate populations during the midnight to noon period.
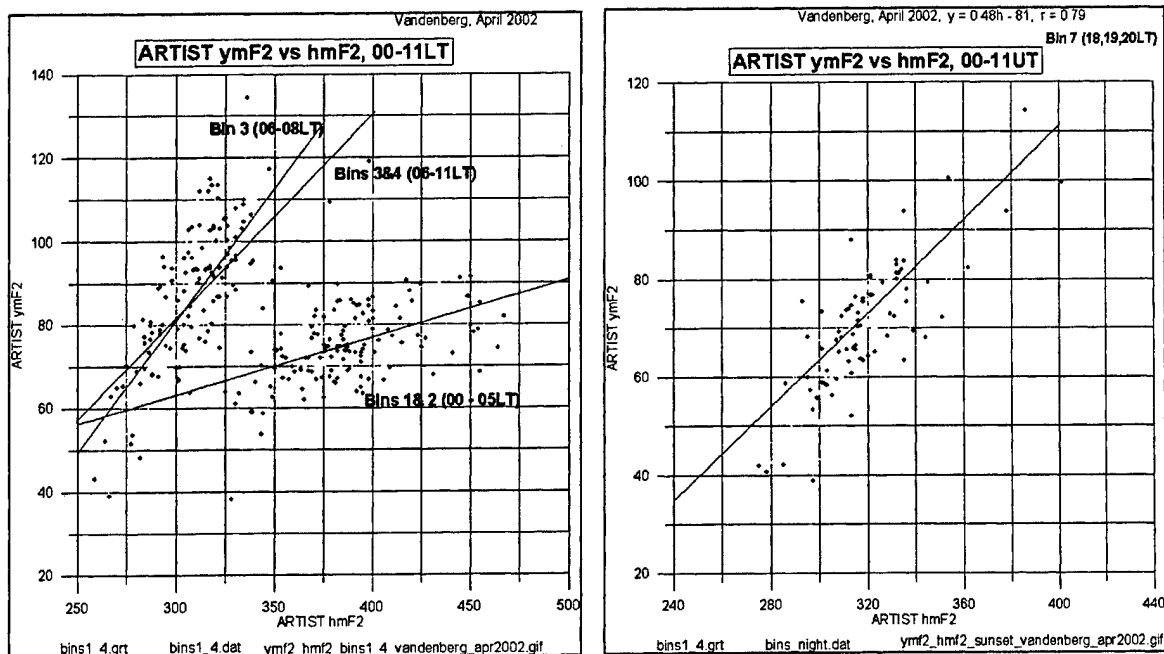
Figure B-18: Corresponding Values of ymF2 and hmF2, Vandenberg, April 2002

The straight lines are the LSF lines for the indicated time intervals (produced by special runs of *analyze_profiles.for*). The highest correlation in this interval for the left-hand plot occurs for bin 3 (06-08LT), or post sunrise.

As with the Jicamarca data, the correlations can be interpreted in terms of the variations of the three parameters hmF2, ymF2 and h(0.5NmF2). The diurnal variations of the three parameters are shown in *Figure B-19*.
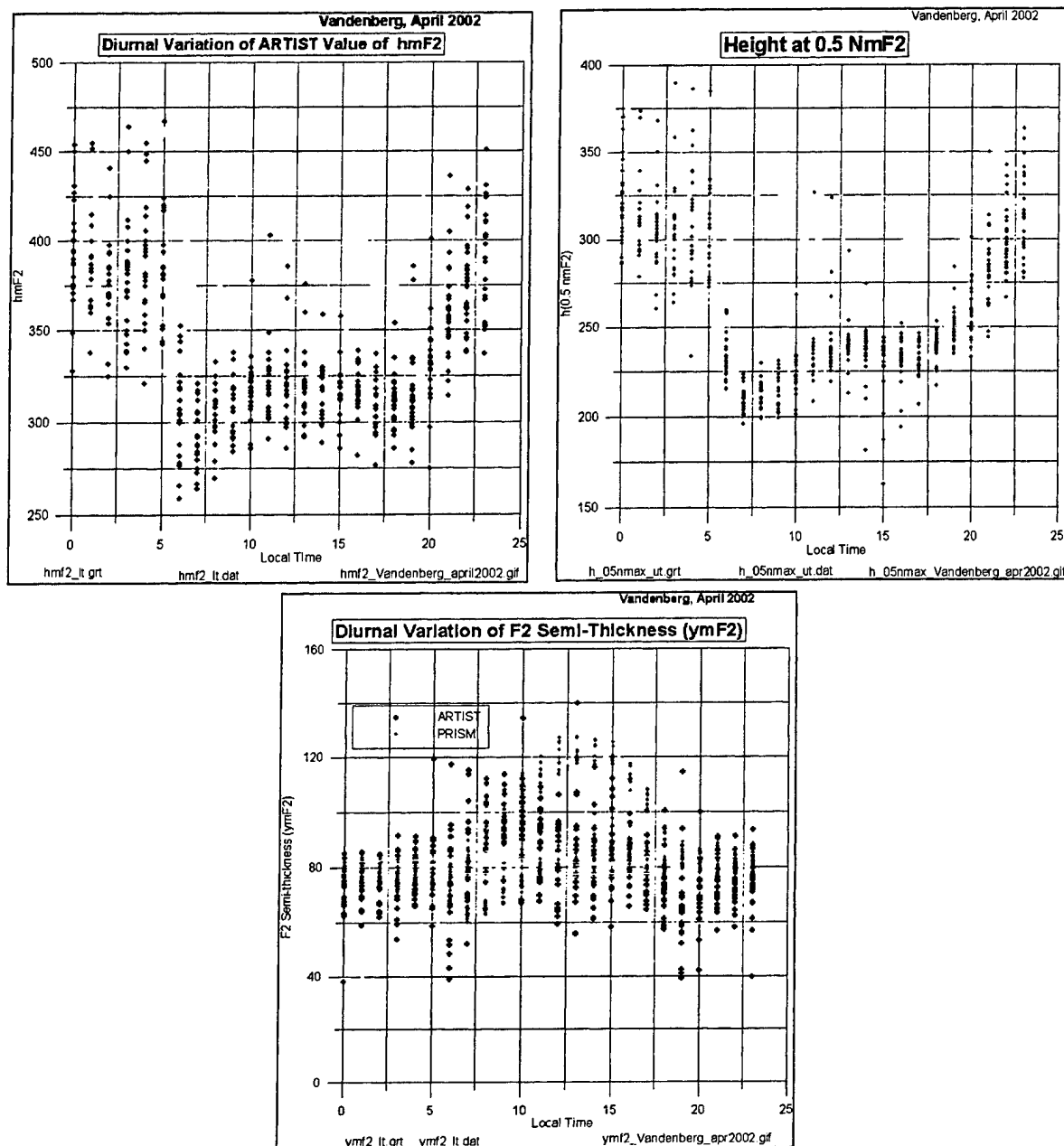
59

Figure B-19: Diurnal Variations of hmF2 and h(0.5nmF2), Vandenberg, April 2002

The highest correlations occur at dawn and sunset. At dawn, ymF2 and hmF2 go up together, while at sunset they go down together.

Implications of PRISM's Pathological Profiles

This section describes some impacts of PRISM's pathological profiles on operational systems such as OpSEND. The discussion is couched in terms of the vertical and oblique incidence ionogram for a 3000km circuit.

Figure B-20 shows the corresponding ARTIST and PRISM electron density profiles and vertical incidence ionograms, for Jicamarca, July 1, 16UT.
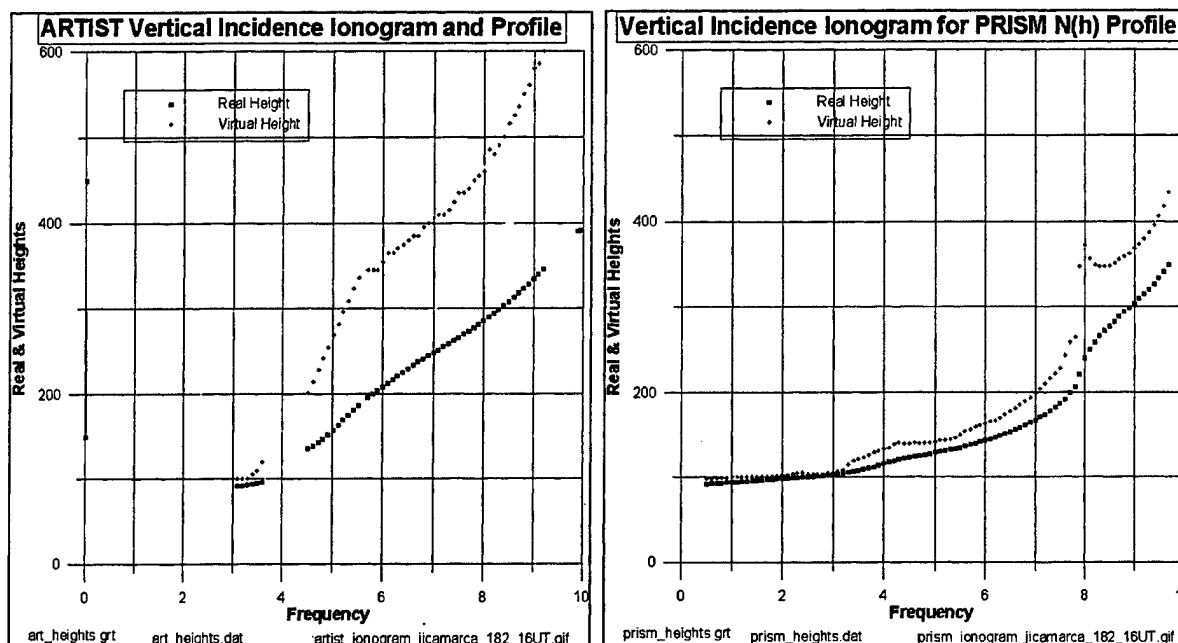

Figure B-20: ARTIST and PRISM Profiles and V.I. Ionograms (Jicamarca, 182/16UT

The ARTIST data was extracted from the SAO file, while the PRISM ionogram was obtained by direct integration of the group refractive index from the base of the ionosphere to the reflection height.

The ionograms (red traces) are obviously completely different, apart from sharing the same value of foF2. The PRISM virtual height trace is far too low, and has a spurious cusp at ~8MHz due to the point of inflection in the profile. The extra points at the ends of the profiles are (foF2,hmF2). The errors in the PRISM ionogram do not warrant detailed calculations.

The incorrect heights at any frequency, fv, in the ionogram would lead to incorrect take-off angles, which could lead to the use of inappropriate antennas. They would also lead to incorrect group paths, which would impact the calculation of the different loss terms along the circuit, leading to incorrect estimates of the signal-to-noise ratio at the receiver.

Another way of comparing the effects of the differences between the two profiles is by comparing the corresponding oblique ionograms, which are shown in *Figure B-21*.
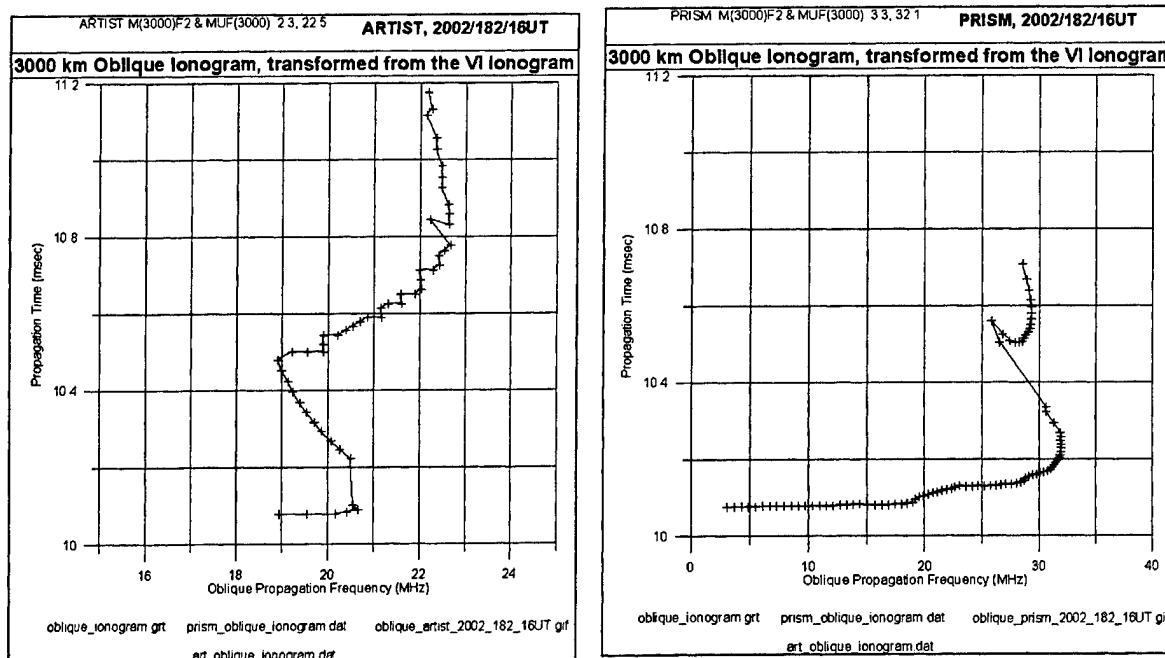
Figure B-21: ARTIST and PRISM Oblique Ionograms for a 3000km circuit.

These ionograms have been obtained by transforming the vertical incidence ionogram to a range of 3000km.

(In this transformation procedure, a point (f_v, h') on the V.I. ionogram is transformed to an oblique frequency of $f_v k \sec \Phi$, and the group path is the time taken to travel the triangular path which has an apogee equal to h'.)

Note: The errors in the PRISM ionogram (for the pathological profiles) are so large that they do not warrant the calculation of multiple-hop traces or X-mode traces, so the plots above do not look much like actual oblique ionograms.

The most important thing to note is the different MUFs for the two ionograms - 22.5 MHz for ARTIST and 32 MHz for PRISM. In other words, PRISM would predict that frequencies up to 32 MHz could be supported on the 3000 km circuit. Errors such as these can lead to inappropriate frequency selection for HF communications, and incorrect skip zones. The predicted skip zone is used in developing propagation tactics to avoid intercept stations.

The multipath spread (in time delay) would also be predicted incorrectly, affecting the signal-to-noise ratios that are required to maintain a required grade of service for HF communications.